Clays and Clay Minerals, Vol. 64, No. 6, 767–787, 2016.

APPLICATION OF MULTIVARIATE ANALYSIS IN THE ASSESSMENT OF CERAMIC RAW MATERIALS

José V. Lisboa[1,*], Fernando Rocha[2], and Daniel P. S. de Oliveira[1]

[1] Laboratório Nacional de Energia e Geologia (LNEG), Mineral Resources and Geophysics Research Unit, Estrada da Portela, Bairro do Zambujal, 2610-999 Amadora, Portugal
[2] Geobiotec, Geosciences Department, University of Aveiro, 3810-193 Aveiro, Portugal

Abstract—The aim of the present study was to discriminate between distinct types of clay units by applying multivariate statistical techniques, which have seldom been applied to the exploitation of ceramic clays. At the outcrop scale, texturally similar argillaceous or clayey layers of different ceramic types cannot be effectively distinguished, which can result in the misuse and loss of raw materials. Representative samples of clayey raw materials from central Portugal Cenozoic deposits with potential use in the manufacture of structural clay products were first assessed for granulometric, mineralogical, chemical, and technological properties. Based on those properties and the use of multivariate statistical techniques, *i.e.*, factor analysis (FA) and cluster analysis (CA), a novel statistical approach that combined all these variable properties was produced. This approach made it possible to distinguish the ceramic suitability and perceive which parameters most influence that suitability. The use of R-mode FA made it feasible to differentiate and group samples based on the most influential variables: the contents of Al_2O_3, Fe, illite, quartz, feldspars, and K_2O. The use of R-mode CA substantiated the FA results in the identification of influential variables, such as Al_2O_3, Fe, and illite. The use of Q-mode CA established two main clusters: clayey-silt samples and sandy and/or feldspathic samples, the clayey-silt samples encompassed three sub-clusters. These three sub-clusters match ceramic types with different suitabilities and relate sample stratigraphic setting to the encompassing stratigraphic units. Diagrams that relate the grain size, the content of different oxides, the content of different minerals, and the plasticity to the ceramic suitability illustrate the CA groupings. An adequate blend of sand and clay for red stoneware (bricks and tiles) manufacture was indicated as a major requirement for most raw materials of the clayey-silt cluster. Raw materials represented by the sandy and/or feldspathic cluster can either be used to blend with materials that lack sand or to blend with excessively plastic samples.

Key Words—Ceramic Behavior, Clay, Cluster Analysis, Factor Analysis, Mondego Planation, Structural Ceramics.

INTRODUCTION

Multivariate statistical analysis is broadly used in clay science for various applications. In the investigation of ceramic raw materials, these techniques have also been applied to assess deposits and manufactured products (*e.g.* Mazzoleni and Summa, 1996; Galan *et al*., 1998; Cravero *et al*., 2010; Marques *et al.*, 2011; Agha *et al*., 2012), more frequently applied in the study of archaeological ceramics (*e.g.* Zhu *et al.*, 2004; Braekmans *et al*., 2011; Montana *et al.*, 2011; Kramar *et al*., 2012; Maritan *et al.*, 2015), but has seldom been used to assess ceramic raw materials for exploitation (*e.g.* Oliveira *et al.*, 1980; Decleer *et al.*, 1981; Dondi, 1999). In these studies, multivariate statistical tools, mostly factor analysis, have been applied to mineralogical, geochemical, textural, and stratigraphic data and variables, but less frequently used for technological variables/data (Galan *et al.*, 1998). Clay resources occur mainly in Meso-Cenozoic terrains of the Lusitanian basin in western and southern Portugal. Outside the Lusitanian basin, the clay resources occur in interior basins, such as the study area (Figure 1, I.). The ceramic industry, which established there at the beginning of the XXth century, is based on the production of structural clay products (270,000 t in 2010) and although the potential area where raw materials occur is large, the pits and plants are dispersed. This is attributed to the lack of data on the location and types of clay deposits, which occur in two formations that have similar lithofacies at the outcrop scale, and thus make differentiation between the two formations difficult. In a novel approach, the applied methodology was based on investigating the relationships between stratigraphic, compositional, and

* E-mail address of corresponding author:
vitor.lisboa@lneg.pt
DOI: 10.1346/CCMN.2016.064040

This paper is published as part of a special section on the subject of 'Developments and applications of quantitative analysis to clay-bearing materials, incorporating The Reynolds Cup School', arising out of presentations made during the 2015 Clay Minerals Society-Euroclay Conference held in Edinburgh, UK.

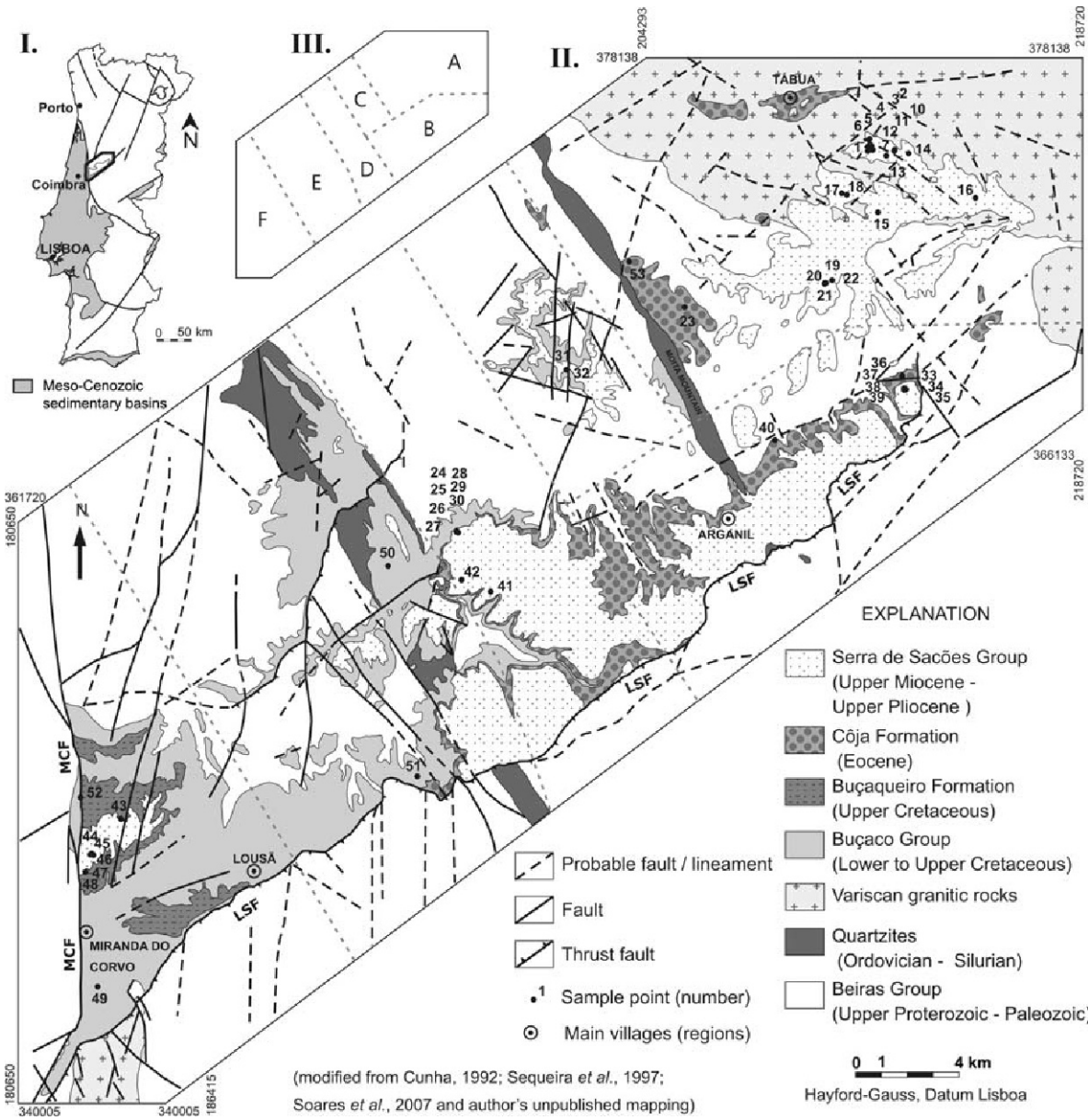

Figure 1. Geological setting of the study area in the Mondego planation (modified from Lisboa *et al.*, 2015) showing: (I) Meso-Cenozoic terrains and study area location (rectangle) in Portugal; (II) sample locations (*LSF*: Lousã- Seia fault; *MCF*: Miranda do Corvo fault); and (III) regions of the Mondego planation: *A*- Tábua, *B*- Coja, *C*- Sanguinheda, *D*- Santa Quitéria, *E*- Lousã, and *F*- Miranda do Corvo.

technological data from a collection of argillaceous samples. This approach was expected to reduce the complexity of the multiple variables that characterize the materials and differentiate deposits with distinct ceramic potential and to group and sort clay stockpiles. Specific aims of this study were: to identify parameters which enhance sample discrimination, to balance relationships between parameters, to group samples using cluster analysis based on the suitability for the manufacture of different ceramic building bodies, and to demonstrate that the method is useful for large numbers of samples.

Attempts have been made to distinguish and rank the suitability of ceramic raw materials for different uses. Various charts and diagrams for raw material classification have been proposed and some have been widely used, especially classifications that use grain size (Winkler, 1954) and mineralogical and chemical parameters (Fabbri and Fiori, 1985; Fiori *et al.*, 1989; Fabri and Dondi, 1995). Regardless of the recognized utility, the diagrams are generally limited by only considering one type of variable (chemical, mineralogical, or other) regardless of interrelationships between the variables.

https://doi.org/10.1346/CCMN.2016.064040 Published online by Cambridge University Press

The classifications that result are only supported by specific variables and thus do not truly reflect the suitability of the material. The proposed method allows a substantial number of interrelated variables to be considered, which improves the suitability classification because it can compare the similarity of whole datasets.

STUDY AREA AND GEOLOGICAL SETTING

The study area is located in the central zone of Portugal, east of Coimbra and west of the Portuguese Central Mountain range. The area consists of a large polygenic planation surface (Mondego planation surface) that truncates Precambrian and Paleozoic age metasediments (Beiras Group) and Variscan granitoids. Continental fluvial and alluvial deposits (Cretaceous and Cenozoic age) were partly preserved in tectonically depressed areas, which are confined by two major faults: the Miranda do Corvo and Lousã-Seia (Figure 1, II). The Cretaceous age deposits include kaolinite-rich feldspathic sands that constitute the Buçaco Group (Albian to Upper Campanian), which is unconformably overlain by the Buçaqueiro Formation (Campanian to Paleocene) (Cunha, 1999, 2000). The Cenozoic infilling is siliciclastic and unconformably overlies either the Cretaceous sediments or the Hercynian basement. The older unit is the Coja Formation (middle Eocene to Oligocene) (Cunha and Reis, 1991; Pais *et al.*, 2013). Upper Miocene to Pleistocene sediments comprise a sequence (340 m thick) mainly represented by conglomeratic and clayey facies, which are interpreted as alluvial fan deposits along tectonic scarps (Serra de Sacões Group) and include Campelo, Telhada, and Santa Quitéria formations from the base upward (Cunha, 1999; Pais *et al.*, 2012, 2013).

Raw materials that are used in structural ceramics occur in the Coja and Campelo formations (Lisboa, 2009, 2014; Lisboa *et al.*, 2013). Cunha (1992, 1999) distinguished two members in the Coja Formation that are separated by an unconformity: the lower member consists of massive arkoses, and the upper member has facies variations but encompasses massive lutites (*i.e.* mudstones). The Campelo Formation (Upper Tortonian to Messinian) consists of alternating conglomeratic shale layers and lutites, which provide the main supply of clays used for structural ceramics in the Mondego planation. The lutitic facies of both formations probably have the same source in terms of lithology and recycled sediments of the Hesperian massif (Lisboa *et al.*, 2015) and so, despite a slight compositional difference, the formations are texturally difficult to distinguish in the field.

METHODOLOGY

Sampling, sample distribution, and analytical procedures

Fifty-one samples of ceramic raw materials were collected in pits and from outcropping clay layers (Figure 1, II). For work organization, the samples were geographically grouped into the 6 regions of the Mondego planation (Figure 1, III, and Table 1). In the study, grain size, mineralogy, and technological variables were statistically assessed. The >62 μm and <2 μm fraction grain sizes were statistically assessed, but the 2−62 μm fraction (*i.e.* silt) was complementary to the <2 μm and >62 μm fractions and more strongly deviated from the normal. The 2−62 μm fraction, therefore, was excluded from the statistical assessment.

Grain-size distribution was determined using a Coulter LS 130 laser diffraction particle size analyzer (Beckman Coulter, Inc., Brea, California, USA) on the 0.1 to 63 μm fraction and by wet sieving the coarser fractions according to the American Society for Testing and Materials (ASTM) C 371-09, (2014) standard. Mineralogical analyses were made using X-ray diffraction (XRD) and by simultaneous differential thermal (DTA) and thermogravimetric (TGA) analysis and dilatometry. For the bulk sample XRD analyses, the samples were dried in a kiln at 40ºC, ground with an agate mortar and pestle, and passed through a 200 mesh sieve (<75 μm). About 0.5 g of the samples (*i.e.* randomly oriented powder mount) were packed into standard aluminum sample holders. The <2 μm fractions were separated from bulk samples using the following method: approximately 50 g of each sample was weighed

Table 1. Mondego planation regions and geological units attributed to the collected samples.

Regions	Geological formations				
	Buçaco Group	Buçaqueiro Fm.	Coja Fm. (lower member)	Coja Fm. (upper member)	Campelo Fm.
A – Tábua			6, 7, 18, 21	3, 4, 5, 11, 12, 16, 19, 20, 22, 23, 53	1, 2, 10, 13, 14, 15, 17
B –Coja			35, 39	33, 34, 36, 37, 38, 40	
C –Sanguinheda				31	32
D – Santa Quitéria				27, 28, 29, 30	24, 25, 26, 41, 42
E – Lousã	50			51	
F – M. Corvo	49	43, 52			44, 45, 46, 47, 48

https://doi.org/10.1346/CCMN.2016.064040 Published online by Cambridge University Press

and placed in 1000-mL flasks with 600 mL of distilled water and 10 mL of dispersing agent (solution of 35.7 g of sodium hexametaphosphate and 7.4 g of sodium carbonate in 1 L of distilled water) were added. The suspensions were mechanically stirred at about 20 rotations per min for approximately 16 h. After the material was stirred and the suspended particles were allowed to settle for 3 h and 50 min (Stokes Law), a 20 mL pipette was placed at a depth of 5 cm in the suspension and the clay fraction was siphoned off. About 20 mL of suspension with the <2 μm fraction was placed in a test tube and centrifuged at about 2400 × g for up to 1 h to sediment the suspended solids. Two oriented slides per sample were prepared as follows: the <2 μm sedimented solids at the bottom of the test tubes were mixed with a stick and some of the material was removed using a pipette and was applied to one end (edge) of a glass slide. Subsequently, the <2 μm samples were rubbed from the edge of the glass slides to about 2/3 of the slide surface using a stick until smooth and homogeneous surfaces were produced on the slides. The clay covered slides were air dried at room temperature to facilitate orientation of lamellar clay minerals or tabular crystals. The sample slides were dried at 60ºC prior to X-ray diffraction analysis. The X-ray diffraction (XRD) patterns of the oriented clay slides were obtained using a Phillips diffractometer (Phillips Analytical, Almelo, The Netherlands) equipped with a PW1830 generator, a PW1820 vertical goniometer with Bragg Brentano geometry, a 0.5º divergence slit , a 0.5º receiving slit, 1º anti-scatter slits, a curved graphite monochromator, and a 2.7 kW Co (λ = 0.154 nm) tube. The X-ray tube voltage and current were 40 kV and 40 mA, respectively. All samples were scanned from 2º to 80º2θ at 1º2θ per min. The data were processed using the PW1877 Automatic Powder Diffraction program version 3.6 h (Phillips Analytical, Almelo, The Netherlands). Thermogravimetric (TG) and differential thermal analyses (DTA) were run using a Shimadzu DTG-50 furnace and a Shimadzu TA-50 WSI thermal analyzer (Shimadzu Corporation, Kyoto, Japan). Dilatometry measurements were carried out using an Adamel Lhomargy DI.10 Modèle 1 dilatometer (Adamel Lhomargy SAS, Roissy en Brie, France) using alumina as reference material. Qualitative and semiquantitative mineralogical analyses followed the criteria recommended by Schultz (1964), Thorez (1976), and Brindley and Brown (1980). The relative mineral abundances were estimated from the relative height/area proportions of the main XRD reflections as described in Lisboa *et al*. (2015). Bulk samples were analyzed for major elements using X-ray fluorescence (XRF) spectrometry on fused discs (1150ºC) using a Phillips PW 2404 (PANalytical, The Spectris Technology, The Netherlands) equipped with a 4 kW Rh X-ray tube. The Mn and Fe contents were measured using the Rh X-ray tube operated at 50 kV and 60 mA. The other elements were determined using the Rh X-ray tube operated at 30 kV and 100 mA. The accuracy and precision were 1% and 5%, respectively, for all major elements in general. Loss On Ignition (LOI) was determined by heating at 1050ºC for 1 h. The pH was determined following the ASTM D 4972-13 (2013) method using a Sentron 2001 pH System instrument (Topac Inc., Cohasset, Massachusetts, U.S.A.). For the technological characterization, a few relevant properties of the samples were studied. The plasticity properties were obtained by determining the Atterberg limits: liquid limit (LL), plastic limit (PL), and plasticity index (PI). The plasticity index was calculated as the difference between the LL and PL of the clays. Liquid limit and plastic limit tests were carried out using a Casagrande apparatus (Model 22-T0030/F, Ceramic Instruments S.R.L., Sassuolo, Italy) following the ASTM 4318-10 (2010) method. Color was determined based on optical reflectance in the visible zone using a DR colorimeter. A Lange Micro Color Data Station (Braive Instruments, Liege, Belgium) was used to measure color on both unfired and fired powdered samples (<62 μm). The CIE L*a*b* coordinates were estimated: brightness (L*), red/green (a*), and yellow/blue (b*) (CIE, 1978). In order to determine other technological properties, clay prismatic test-pieces (trapezoidal section 2.3 cm × 2 cm × 1.5 cm and 26 cm long) were shaped by extrusion. Unfired samples were characterized by measuring the dry shrinkage using the ASTM C 326-82, 1997 method and the dry bending strength using the ASTM C 689-93, 1997 method. All samples were fired in an electric oven (Fornocerâmica, model KS63/1400ºC, Fornocerâmica, S.A., Leiria, Portugal) at a temperature of 900ºC. According to significance, selected samples were fired again at 1000ºC and 1100ºC, but the data for 1000ºC and 1100ºC were consequently not considered in the statistical study. The firing profile consisted of four different stages: 10ºC/min up to 60ºC, 11ºC/min from 60 to 110ºC, 4ºC/min from 110 to 580ºC, and 2ºC/min from 580ºC to the maximum temperature. The specimens were maintained at the maximum temperature for 15 min. After equilibrating at the maximum temperature, the samples were cooled in the furnace to room temperature. Water absorption (ASTM C 373−88, 1999), firing shrinkage (ASTM C 326-82, 1997), and bending strength (ASTM C 674-89, 1999) were determined on the fired products. The water absorption values were determined by measuring the mass differences between the as-fired and the water saturated samples (immersed in boiling water for 2 h, cooled for 3 h, and the surface swept with a wet towel). To determine the linear firing shrinkage, a 10 cm line mark was molded into the specimens and variations in length were measured after the samples were fired using the formula $[(l_d - l_f)/l_d] \times 100$, where l_d and l_f are the measured length of dried and fired specimens. The bending strength was measured using the three points technique in a Zwick Z010 (Zwick

https://doi.org/10.1346/CCMN.2016.064040 Published online by Cambridge University Press

GmbH & Co, Ulm, Germany) apparatus operated at 2 kN, 10 mm/min, and was calculated using $BS=3FL/(B+b)h^2$, where F = breaking load (kg/cm^2), L = distance between supports (cm), B = larger base width (cm), b = smaller base width (cm), and h = specimen thickness (cm).

Descriptive statistics and correlations

To better understand the analytical data structure, the data distributions of 41 variables, which encompassed grain size, chemical, mineralogical, and technological parameters were first tested using descriptive statistics. The kurtosis and skewness were the preferred tests of the normality of each variable data set before any correlations were assessed and before use of multivariate analysis (Zhou *et al.*, 2007). Given that most variables in data sets are not normally distributed and a significant number of variables must be expressed in percentages, therefore, standardization was applied to overcome this problem. Using the logarithm of variables is another widely used method to normalize data (Kowalkowski *et al.*, 2006; Papatheodorou *et al.*, 2006; Zhou *et al.*, 2007), but logarithms could not be applied in the present study because several of the skewness and kurtosis values were negative. The Spearman rank correlation coefficient was used to assess the relationships between variables instead of linear correlation (Bundy *et al.*, 1966; Davis, 1986; Rollinson, 1993; Singh *et al.*, 2004) because the Spearman rank correlation coefficient is less sensitive to factors, such as outliers and non-normal distributions.

Multivariate analysis

Data preparation. A major difficulty in applying classical statistical methods is that a normal distribution of data is assumed, which seldom occurs with geochemical and technological data. Such data are spatially dependent and are often based on inaccurate measurements (Reimann and Filzmoser, 2000). Multivariate analysis techniques were applied using STATISTICA software version 6.1 (Statsoft, 2001). To ensure that the statistical methods chosen were applicable, variables with distributions closer to normal distributions were selected. Different combinations were tested and selected when the result was consistent with stratigraphic, textural, chemical, mineralogical, and technological criteria. The need to transform data series depends on the degree of asymmetry of the the data and on the data, but no consensus exists as to applicability (Child, 1970; Gorsuch, 1974). In this context, after the data was assessed using descriptive statistics and correlations, standardization was tested. To effect standardization of the data, the distribution average was subtracted from each observation and divided by the standard deviation of the distribution. A statistical multivariate analysis of robust data sets helps to set up comprehensive models for geotechnical and technological (such as ceramic) properties (Galhano *et al.*, 1999; Zorski *et al.*, 2011). The Principal Components method identifies, on one hand, the variables that better characterize each formation/deposit and, on the other hand, finds correlations between the variables (Cravero *et al.*, 2010).

Factor analysis (FA). An R-mode FA analysis was performed on the data of 12 variables in order to group the mutually correlated variables and to quantitatively evaluate the clustering behavior. The number of observations (samples) is one of the limitations in obtaining reliable principal components and the sample number should be >100 (*e.g.* Gorsuch, 1983; Stevens, 1986). Published research, however, supports (*e.g.* Kumru and Bakaç, 2003; Papatheodorou *et al.*, 2006; Zhou *et al.*, 2008) the use of FA to produce credible results when the number of observations is in the same range as the present study or lower.

Cluster analysis (CA). Cluster analysis is a technique for agglomerative hierarchical classification (Everitt, 1977), which has been a preferred aid to highlight relationships between variables, to organize data, and to understand the distribution of samples. The Pearson correlation coefficient was used for group definitions. After comparing the results obtained using different aggregation criteria, the Ward (1963) criterion was chosen. The obtained results were advantageous in comparison to the other criteria tested, though with minor differences between the results. The resultant cluster structure depended on the variables chosen and several combinations of all types of variables were tested to avoid redundancy.

RESULTS

Analytical procedures

Compositional characterization. The data indicate that silt size particles (sand = >63 μm, silt = 2−63 μm, clay = <2 μm) were predominant for most samples, which were fitted into two major granulometric (or textural classes) sample groups (Shepard, 1954). One group included silt and clayey silt and the other group encompassed sandy silt, silty sand, and sand (Figure 2). The mineral analyses of the clayey raw materials (Table 2) revealed that the bulk samples contained similar proportions of quartz, illite/mica, and, to a lesser extent, kaolinite. Smectite or mixed-layer smectite/chlorite was observed in most samples, often in significant amounts. Chlorite was detected in a small number of samples. The occurrence of a 14 Å (001) diffraction peak in untreated and heated oriented samples (no (002) 7 Å and (004) 3.5 Å diffraction peaks after heating at 550ºC) that occasionally had an increased intensity after heating indicates low-iron chlorite varieties (Thorez, 1976; Brindley and Brown, 1980), but the diffractograms were not sufficient to allow any other conclusions to be made about the nature of the chlorites. Feldspars occurred in almost all

https://doi.org/10.1346/CCMN.2016.064040 Published online by Cambridge University Press

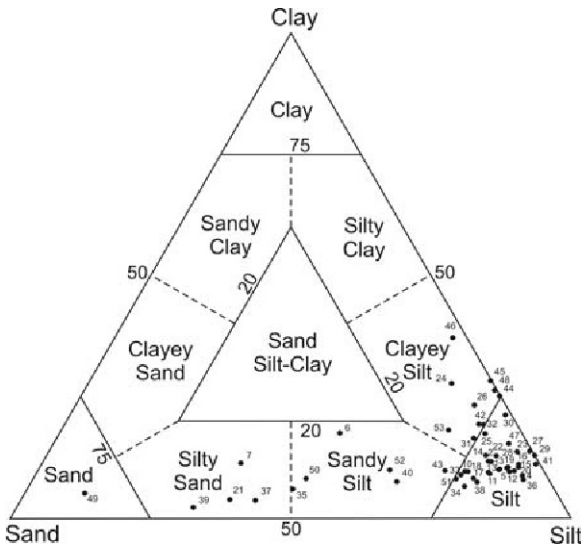

Figure 2. Classification of raw material samples based on proportions of sand, silt, and clay (Shepard, 1954).

samples and hematite was recognized to a limited extent. The semi-quantitative mineralogical compositions of the clay fractions naturally reflected a strong enrichment in clay minerals (total content of non-clay minerals < 10%, in most samples), which was mainly illite-kaolinite or illite-kaolinite-smectite. These data were further supplemented with differential thermal (DTA) and thermogravimetric (TGA) analyses (Figure 3). The DTA curves exhibited endothermic peaks from about 50ºC to about 240ºC, during which water was lost with intense peaks due to the predominantly illitic and/or smectitic composition. The endothermic reactions between 294ºC and 311ºC were explained by the dehydroxylation of iron (oxyhydr)oxides (Singer and Singer, 1963; Jouenne, 1975). The DTA peaks between 485 and 557ºC were due to dehydroxylation (Mackenzie, 1957, 1962; Blazek, 1972). The 485−516ºC peaks (majority of samples) were related to illite/mica and/or smectite and the up to 557ºC peaks were attributed to kaolinite. A weight-loss peak in the TGA curve between 480 and 560ºC was mainly related to illite/mica and kaolinite and partly due to smectite and the intensities were dependent on the mineral contents (Mackenzie, 1962). Related to the high quartz content of most samples, characteristic quartz endothermic peaks (573ºC) (Mackenzie, 1962) were observed at 573-579ºC (Figure 3a), except for a few samples (27, 44, 45, 46, and 48) due to the low quartz contents (Figure 3b). Exothermic peaks observed at a temperature between 970-995ºC were due to the modification of metakaolinite to a new intermediate phase prior to mullite formation (Mackenzie, 1962). In a significant number of samples, an exothermic peak at 896-925ºC was frequently preceded by an endothermic peak characteristic of illite/mica and depended on the mineralogical composition, which can also be attributed to smectite (Mackenzie, 1962; Singer and Singer, 1963).

Table 2. Mineralogical (bulk sample/<2 μm fraction; data in % for both fractions) and chemical compositions of bulk sample and <2 μm (%). The abbreviations are: Ilt = illite; Kln = kaolinite; ML = mixed layer minerals; Sme = smectite; Chl = chlorite; Qz = quartz; Fsp = feldspar; Hem = hematite; LOI = loss on ignition; $pH_{1'}$ = after 1 min; $pH_{15'}$ = after 15 min; and tr = trace.

Sample	1	2	3	4	5	6	7	10	11	12	13	14	15	16	17	18	19	20	21	22	23	24	25	26	27
Ilt	30/34	35/50	36/44	32/40	50/52	7/18	5/13	37/52	37/37	31/27	38/39	27/42	32/46	36/38	43/44	35/38	28/36	29/33	17/22	32/46	43/33	36/70	23/40	33/45	38/55
Kln	24/64	18/47	14/28	11/24	15/33	17/54	14/67	23/46	16/30	11/14	24/49	30/56	22/51	13/23	28/54	20/38	16/37	11/19	16/44	9/17	30/54	13/25	11/20	9/20	3/1
ML			3/6						14/27	22/56				9/33									17/34	9/10	30/25
Sme				14/28	3/11	5/19	3/7				2/9					7/21	9/24	14/43	4/18	13/29	4/11				5
Chl																									
Qz	43/1	43/2	40/19	34/8	28/4	50/8	61/13	34/1	27/6	29/3	33/2	38/1	40/3	39/6	26/1	29/3	41/3	42/5	41/15	42/8	20/2	44/3	43/5	40/22	18/5
Fsp	1/tr	2/tr	5/1	8/tr	2/tr	20/1	17/tr	3/tr	6/tr	7/tr	2/tr	2/tr	2/tr	3/tr	2/tr	9/tr	3/tr	4/tr	22/1	3/tr	2/-	3/1	3/tr	6/2	11/5
Hem	2/1	2/1	2/2	1/-	2/tr	1/-		3/1			1/1	3/1	3/tr		1/1		3/-			1/tr	1/-	4/1	3/1	3/1	-/4
SiO_2	65.57	64.73	63.77	61.50	54.62	68.80	75.80	63.74	62.21	61.49	67.1	63.06	61.59	61.68	66.99	64.78	61.21	60.04	77.94	70.35	59.15	64.47	66.36	61.23	55.56
Al_2O_3	18.45	18.33	17.04	17.19	22.35	15.16	12.00	17.93	17.35	16.74	16.74	19.14	20.03	17.86	17.41	16.98	18.13	17.52	11.71	13.00	22.74	17.32	15.68	17.46	15.72
Fe tot	5.81	6.38	6.37	6.52	7.86	2.89	2.03	6.74	6.26	5.99	5.51	6.61	6.11	6.20	5.08	4.35	6.87	5.96	1.83	5.34	3.76	6.39	5.67	6.86	5.49
MnO	0.02	0.04	0.03	0.11	0.20	0.03	0.02	0.04	0.04	0.04	0.02	0.02	0.02	0.04	0.03	0.03	0.02	0.04	0.02	0.02	0.01	0.05	0.02	0.04	0.03
CaO	0.04	0.04	0.04	0.05	0.04	0.05	0.05	0.04	0.11	0.13	0.04	0.04	0.05	0.16	0.04	0.14	0.04	0.07	0.04	0.11	0.06	0.06	0.08	0.09	0.08
MgO	0.25	0.36	0.93	1.59	1.00	0.91	0.50	0.58	1.56	1.88	0.58	0.32	0.46	1.60	0.53	1.16	0.77	1.66	0.36	0.80	0.88	1.04	1.36	1.46	5.32
Na_2O	0.2	<0.20	0.20	0.48	0.20	0.29	0.80	0.20	0.20	0.29	<0.20	<0.20	0.47	0.65	<0.20	0.24	0.20	0.20	<0.20	<0.20	<0.20	<0.20	<0.20	0.53	0.20
K_2O	2.18	2.83	3.1	2.97	3.91	3.52	2.75	2.93	3.26	3.08	2.69	2.40	2.81	3.35	2.69	3.64	2.37	3.04	3.11	2.08	2.91	3.05	2.56	3.26	3.31

https://doi.org/10.1346/CCMN.2016.064040 Published online by Cambridge University Press

TiO_2	1.15	1.09	0.99	0.90	0.81	0.57	0.39	1.00	0.88	0.83	1.01	1.25	0.96	0.92	1.17	0.88	0.96	0.80	0.29	0.90	0.76	0.81	0.86	0.89	0.77
P_2O_5	0.06	0.09	0.06	0.07	0.04	0.07	0.07	0.08	0.07	0.04	0.07	0.12	0.11	0.07	0.08	0.09	0.04	0.05	0.05	0.08	0.04	0.09	0.06	0.08	0.04
LOI	6.19	5.87	7.29	8.32	9.02	7.25	5.19	6.38	7.91	9.15	5.95	6.58	7.13	7.20	5.83	7.35	9.32	10.52	4.31	7.23	9.40	6.65	7.07	7.81	13.33
$pH_{1'}$	4.57	5.22	6.07	6.37	4.84	5.96	5.30	6.28	6.75	6.69	5.44	4.27	4.91	6.38	5.71	6.02	5.57	5.70	5.32	5.24	5.14	7.55	6.00	8.29	8.51
$pH_{15'}$	4.57	4.81	5.86	6.34	4.85	5.84	5.14	6.00	6.47	6.54	5.26	4.26	4.85	6.09	5.50	5.51	5.34	5.40	5.13	4.95	4.98	7.38	5.69	8.12	8.58

Table 2 (continued)

Sample	28	29	30	31	32	33	34	35	36	37	38	39	40	41	42	43	44	45	46	47	48	49	50	51	52	53
Ilt	35/51	40/51	54/71	45/51	39/67	20/37	20/35	5/29	40/53	28/25	32/40	24/27	7/13	41/42	33/60	6/36	37/50	40/54	51/72	48/57	61/52	3/13	11/7	8/10	25/30	10/30
Kln	8/9	9/17	8/12	9/15	15/28	4/34	3/28	3/20	4/10	7/14	2/18	5/34	-/22	8/12	9/18	28/59	28/42	34/37	24/27	10/17	24/35	5/80	28/90	8/23	37/68	16/34
ML	16/30	18/16	8/10							9/57	6/23	-/12		12/34				5/7		4/18	-/8					
Sme				12/27		4/2	5/25	3/35	6/15				8/45		5/16		4/5							17/56		8/26
Chl						11/25	11/8	-/6	13/18		11/8															
Qz	31/9	25/14	19/3	30/6	40/3	54/2	28/4	63/9	28/3	38/4	30/10	42/20	69/20	31/11	44/5	64/4	23/3	18/2	20/1	29/7	14/5	74/6	61/3	29/11	34/2	62/10
Fsp	9/1	7/1	11/4	3/1	3/1	6/tr	31/tr	26/1	9/1	18/tr	19/1	23/7	14/-	4/1	4/1	-/tr	6/tr	3/tr	3/tr	7/1	1/tr	16/1		38/tr	4/tr	2/tr
Hem	1/-	1/1		1/tr	3/1	-/tr	1/-					1/-	2/-	4/-	5/-	2/4	2/tr	-/tr	2/tr	2/tr		2/-				2/-
SiO_2	61.34	61.41	51.34	65.57	66.12	69.80	61.02	77.35	61.34	73.10	62.51	74.25	73.03	61.64	63.76	77.98	53.2	49.79	49.83	59.31	52.79	84.52	78.12	65.17	64.78	73.67
Al_2O_3	16.67	17.89	20.36	16.20	17.73	12.76	17.61	9.71	18.49	12.99	16.9	13.54	12.95	17.04	16.67	12.18	23.1	23.09	23.73	18.97	22.67	8.08	13.94	15.91	20.71	12.17
Fe tot	6.31	5.97	6.47	5.72	5.49	5.80	5.69	2.50	5.99	2.54	5.36	1.80	2.25	5.92	5.87	3.47	7.00	7.66	8.05	7.02	7.18	1.53	0.95	2.76	2.22	2.75
MnO	0.04	0.04	0.03	0.02	0.02	0.03	0.08	0.02	0.02	0.04	0.10	0.02	0.02	0.02	0.02	0.06	0.02	0.03	0.03	0.05	0.04	0.50	<0.02	0.02	<0.02	<0.02
CaO	0.11	0.10	0.10	0.09	0.04	0.08	0.19	0.13	0.15	0.13	0.24	0.16	0.04	0.09	0.07	0.04	0.07	0.09	0.15	0.10	0.41	0.04	0.04	0.11	0.05	<0.04
MgO	2.25	1.88	3.49	1.10	0.47	1.88	1.97	1.01	1.86	0.99	1.89	0.51	0.84	1.73	1.41	0.10	0.99	0.65	1.62	1.82	1.89	0.09	0.11	0.99	0.43	0.70
Na_2O	0.63	0.53	0.20	<0.20	<0.20	0.77	1.18	1.06	0.20	1.23	1.37	1.50	<0.20	1.10	0.60	<0.20	0.32	0.20	0.20	0.20	<0.20	0.20	<0.20	1.37	<0.20	<0.20
K_2O	3.26	3.57	4.58	2.90	3.14	2.15	3.28	3.25	3.15	4.35	3.64	4.92	1.70	3.36	3.00	0.88	3.65	4.39	5.19	3.94	4.52	2.62	0.73	5.27	3.07	1.33
TiO_2	0.78	0.86	0.79	0.80	1.03	0.73	0.85	0.42	0.85	0.44	0.79	0.42	0.47	0.85	0.79	0.91	0.67	0.54	0.52	0.84	0.56	0.10	0.57	0.45	0.61	0.76
P_2O_5	0.06	0.06	0.03	0.07	0.08	0.08	0.08	0.08	0.08	0.13	0.14	0.10	0.05	0.08	0.08	0.06	0.03	0.05	0.12	0.10	0.07	0.03	0.04	0.11	0.08	0.05
LOI	8.29	7.43	12.45	7.36	5.45	5.62	7.88	4.22	7.64	3.87	6.69	2.63	8.17	8.04	7.30	4.15	10.76	12.07	10.37	7.47	9.58	2.63	5.19	7.53	7.71	8.31
$pH_{1'}$	8.28	8.06	8.61	5.49	5.10	7.45	7.82	8.22	5.96	7.04	7.94	7.87	5.09	5.73	7.39	4.50	5.75	6.49	6.94	7.30	8.38	6.02	4.95	5.12	5.91	4.90
$pH_{15'}$	8.20	7.96	8.56	5.11	4.78	7.65	7.76	8.33	5.90	7.20	7.72	7.90	4.90	5.48	7.42	5.01	5.52	6.36	7.03	7.35	8.36	6.02	4.74	4.83	5.84	4.74

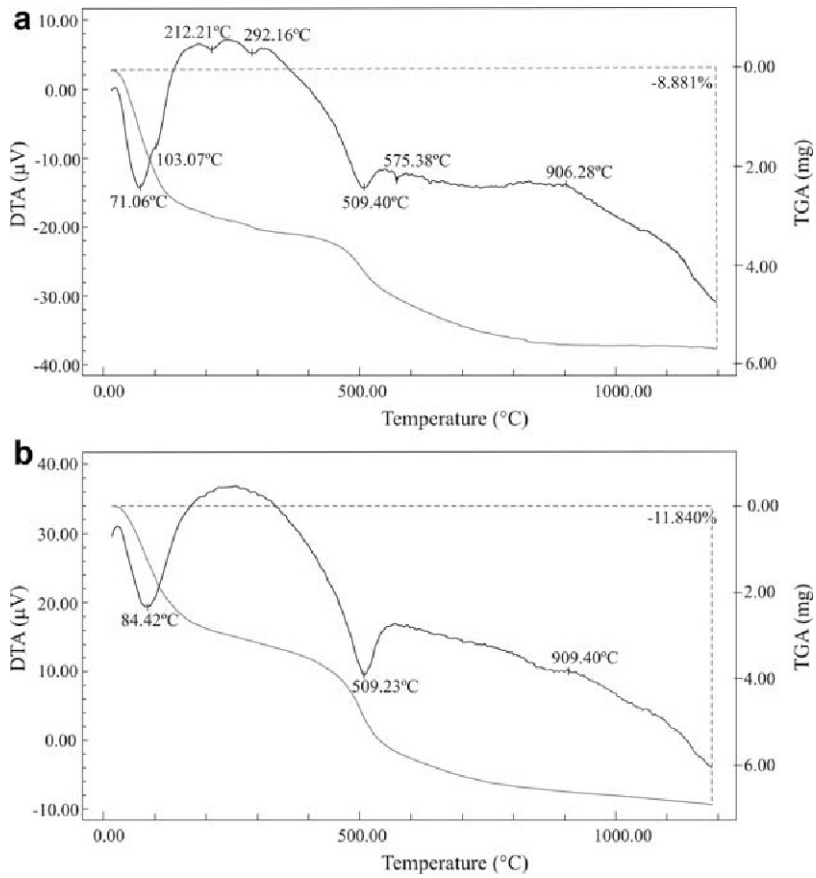

Figure 3. Sample DTA and TGA curves: (a) sample 4 and (b) sample 45.

Dimensional changes observed in the probes after firing can be assigned to four typical thermodilatometric curves (each assigned to a representative sample), which represent the main mineralogical composition types. All samples registered a sharp expansion at 573ºC (α→β-quartz modification) due to the quartz content (Figure 4). Thermodilatometric curve A (sample 14) showed no perceptible shrinkage up to ~120ºC. The expansion up to ~510ºC was followed by slight shrinkage due to kaolinite dehydroxylation and a slight expansion effect between 580ºC and 820−880ºC, which was related to the high illite/mica content (Jouenne, 1975). Above 880ºC, strong shrinkage with a maximum at 950−970ºC was due to sintering and the formation of vitreous phases (Singer and Singer, 1963; Jouenne, 1975). This lithotype encompassed quartz-illite-kaolinite and sparingly abundant smectite or 10/14 Å interstratified clay minerals. Thermodilatometric curve B (sample 19) started with an accentuated shrinkage between 50−100ºC and 150−180ºC shrinkage that depended on smectite and interstratified smectite clay minerals. Following the first shrinkage, a second slight shrinkage occurred at 490-510ºC, which is characteristic of kaolinite (Jouenne, 1975). Above 573ºC (quartz structural modification) an expansion effect was observed up to 830ºC and was attributed to illite/mica. Thermodilatometric curve C (sample 28) had a relatively fast progressive dilatation without significant shrinkage starting at 510ºC (due to small amounts of kaolinite) until the sudden expansion of quartz. Between 845 and 970ºC, strong shrinkage was observed and total shrinkage exceeded 4.2%. Thermodilatometric curve D (sample 46) corresponded to illite-kaolinite samples with a low quartz content. Minor shrinkage up to 175ºC that was mainly related to small amounts of smectite and/or interstratified clay minerals was followed by a slow gradual expansion until further slight shrinkage started at 510ºC, which was interrupted by the dilatation of quartz (573ºC). In this type of curve, the effect of the quartz structure inversion was reduced. A slightly dilatant trend followed and was assigned to illite/mica. Between about 580−820ºC, the sample underwent rapid and pronounced shrinkage after 820ºC. The high illite/mica content caused strong shrinkage above 800ºC and made the shrinkage of kaolinite impossible to distinguish. At about 960ºC, the collapse of clay mineral structures occurred and total shrinkage exceeded 8%. Particular thermodilatometric curves were attributed to a smectitic lithotype (sample 51) and quartzose/feldspathic lithotypes with sparingly abundant kaolinite

https://doi.org/10.1346/CCMN.2016.064040 Published online by Cambridge University Press

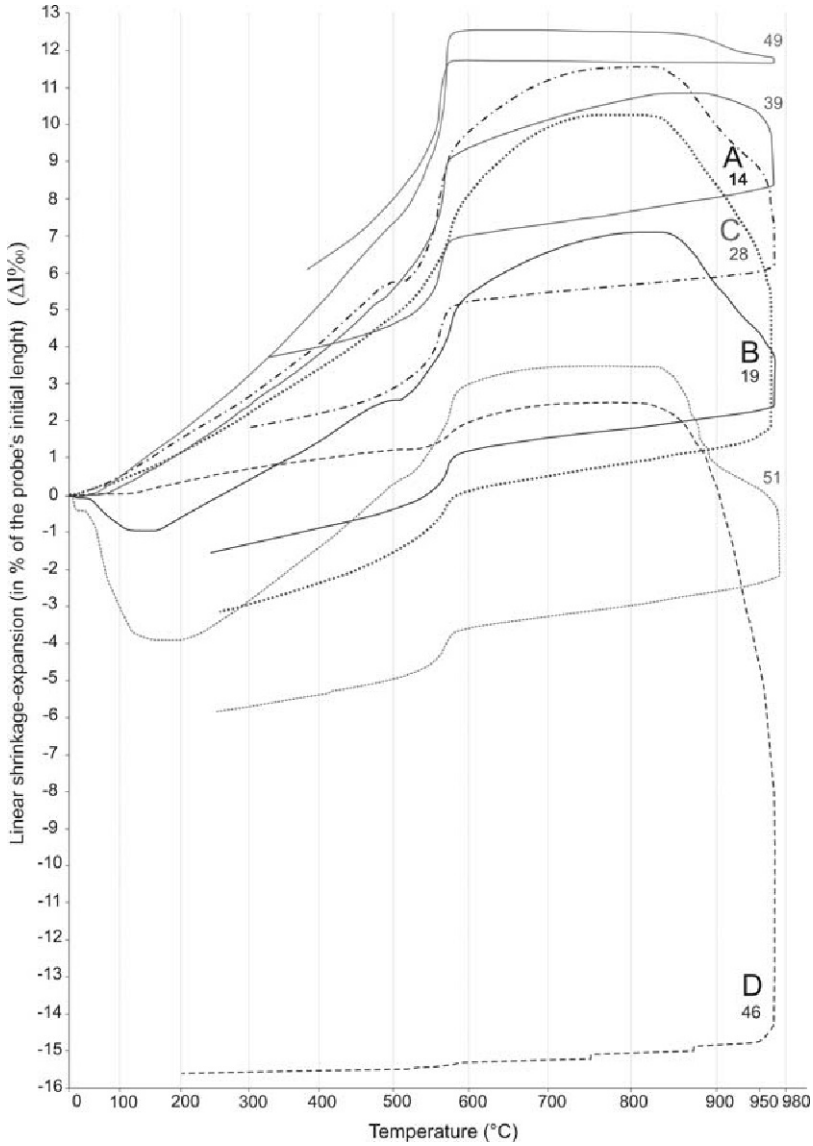

Figure 4. Typical thermodilatometric curves for clay raw materials of types A (sample 14), B (sample 19), C (sample 28), and D (sample 46), and samples 39, 49, and 51.

(samples 39 and 49). Apart from lithotypes represented by curve D, all others required a processing cycle with a moderately decreased rate of firing temperature increase in the 500-600ºC range to compensate for the quartz content and reduce the effects of sudden expansion. Clay raw materials with significant contents of smectite or interstratified smectite clay minerals show a significant first shrinkage, such as type B materials, and require a slow firing temperature on drying up to 200ºC to prevent cracking and/or warping of the ceramic bodies. The major element contents (Table 2) were correlated with the mineralogical characteristics observed. Globally, the chemical analyses showed a high silica content and a relatively low alumina content. The high SiO_2/Al_2O_3 average ratio (3.83) reflects compositions rich in quartz and feldspars. The Fe content of most samples was high (frequently >5%), but hematite and goethite were poorly represented, therefore, Fe was probably associated with amorphous and cryptocrystalline oxides in addition to the Fe in clay mineral structures. The endothermic peaks (294-311ºC) frequently observed in the sample thermograms (except samples 6, 7, 12, 19, 20, 23, 24, 27, 30, 34-38, 40, 44, 45, 49-53) were explained by the dehydroxylation of iron (oxyhydr)oxides, which confirmed the Fe content of the clays. The K_2O was the dominant alkaline oxide due to the illitic composition of most samples and to the presence of K-feldspars. Minor amounts of CaO and MgO reflected the absence of carbonate minerals, gypsum, or talc and the slightly higher MgO content was related to smectite or mixed-

https://doi.org/10.1346/CCMN.2016.064040 Published online by Cambridge University Press

layer smectite. Low TiO_2 values were related to muscovite, kaolinite, and probably vestigial rutile associated with quartz. The Loss On Ignition (LOI) values reflect the hydration water and hydroxyl contents in the clay minerals. The LOI values were generally low due to the high silica and illite content in most samples. The pH values of about 65% of the bulk samples (after 15 min equilibration in water) were <7 (Table 2).

Technological characterization – properties and ceramic behavior.

The CIE Lab parameters of dry sample slabs (Table 3) showed a high dispersion of red (+a*) and yellow (+b*) hues, especially the parameter a* that evidenced the variety of red tonalities in all the samples. After firing at 900ºC, the whiteness (L*) diminished significantly, the yellow hue showed a slight increase with minor changes, and the strong increase in the red hue (Table 3) can be attributed to chromophore elements (Fe and Ti oxides). This corresponded to color changes from light brownish yellow or reddish to darker brownish tonalities. According to the classification by Bruguera (1985) and Caputo (1998), most of the samples had high plasticity indexes (PI >15) and only seven samples had low plasticity indexes (PI <7) (Table 3). Although the raw materials were predominantly silt size, high plasticity was mainly due to the dominance of illite and particularly the presence of smectite, rather than kaolinite. The dry bending strength values obtained (Table 3) were moderate to low (mean BS_d = 20 kg/cm^2), even when the samples with higher sand wt.% were excluded. Low dry bending strength values are usually attributed to high contents of quartz and feldspar in the clay bodies. The observed dry and fired bending strengths at 900ºC (Table 3; mean BS_{900} = 83 kg/cm^2) often satisfied the minimum values of 15 kg/cm^2 and 55 kg/cm^2, respectively, required for the manufacture of bricks (Santos, 1975). The values required for the manufacture of tiles ($BS_d \geqslant 30$ kg/cm^2, $BS_{900} \geqslant 65$ kg/cm^2, Santos, 1975) were attained by samples of the Campelo Formation in the area of Miranda do Corvo and sometimes were achieved by Coja and Campelo formation samples in the Coja, S. Quitéria, and Tábua regions. Overall, the sample wet-to-dry shrinkage values (Table 3) were moderate, but excluded the low values for the sandy samples and the wet-to-dry shrinkage was considered moderate to high. The higher shrinkage values were related either to the greater content of clay minerals or, specifically, with the presence of smectite and illite. In the TGA curves, a significant weight loss up to 220ºC was observed for illite. After firing, dry shrinkage values (Table 3) were, in general, moderate ($LS_{w/d}$ = 2 ± 1%), which was mainly due to the high amounts of non-clay minerals in most samples. Dry-to-fired and wet-to-dry shrinkage were associated with the smectite minerals and due to a higher proportion of clay minerals rather than quartz/feldspar. These characteristics resulted in a slower loss of water. This applies to Miranda do Corvo and S. Quitéria samples, which showed values of dry-fired shrinkage in the same order as the wet-dry shrinkage. Additionally these samples had the highest values of total shrinkage. The significant weight loss (approximately in the 480–560ºC range) of these samples was due mainly to the dehydroxylation of illite and kaolinite (Jouenne, 1975). The Coja Formation samples had higher average total shrinkage values than those of the Campelo Formation and the average total shrinkage at 900ºC was 9 ± 3%. The firing of samples at up to 900ºC provided high water absorption values (Table 3; average value 18%) mainly due to the granulometric characteristics of samples with a low clay content.

Statistical analysis

Descriptive statistics and correlations. The descriptive statistics (Table 4) revealed a high dispersion of the data, but oxides, such as SiO_2 and Al_2O_3, had the lowest coefficient of variation (CV). This denotes a homogeneous distribution of related mineral species within the study area, in particular SiO_2 (CV = 0.12) due to the quartzose composition of most samples. The interpretation of the results did not improve when the variables were standardized, probably due to the heterogeneous composition and ceramic behavior of the samples. As in these conditions, standardization may eventually produce flawed results and, therefore, the untreated data was used. Based on a comparison of the average and median values, as well as the skewness and kurtosis (Table 4), the variable data distributions deviated significantly from the normal (2-63 μm, L^*_{900}, b^*_{900}, and PL) and were rejected for correlation interpretations. The MgO, >63 μm, and $Fsp_{(t)}$ (total feldspars) data distributions did not follow a normal distribution, but were considered because strong correlations were observed. The MgO, >63 μm, and $Fsp_{(t)}$ data distributions were not used in multivariate exploratory techniques, except $Fsp_{(t)}$ which allowed a good discrimination. According to the statistical analyses, the Spearman rank correlation coefficient (95% confidence level) determined for the sample ensemble (Table 5) had significant negative correlations (>|0.60|) for $quartz_{(t)}/Al_2O_3$, $illite_{(t)}/quartz_{(t)}$ as well as SiO_2 with Al_2O_3, LOI, and K_2O, which indicated a strong distinction between sandy and clayey facies and the SiO_2 content was associated with the >63 μm fraction. Positive correlations between Al_2O_3/Fe_{tot}, Fe_{tot}/illite, and clay minerals/Fe_{tot} indicated an association between Fe^{2+} and/or Fe^{3+} and clay minerals. The positive correlation between Fe_{tot} and LOI may indicate that part of the Fe is a component of oxides and oxyhydroxides, as suggested by the DTA curves (Figure 3a). The alkaline earths were usually minor constituents of these clays. A significant part of the Mg^{2+} was incorporated into smectite and interstratified clay minerals, but given that the MgO distribution significantly deviated from the normal, the significance

https://doi.org/10.1346/CCMN.2016.064040 Published online by Cambridge University Press

Table 3. Technological properties of the samples with CIELAB color parameters and whiteness-degree of samples. The abbreviations are: PL = plastic limit; LL = liquid limit; PI = plastic index; BS_d = dry bending strength; $LS_{w/d}$ = wet-to-dry shrinkage; WA_{900} = water absorption; BS_{900} = bending strength at 900 ºC heated samples; $LS_{d/f}$ = dry-to-fired shrinkage $LS_{t\ 900}$ = total shrinkage; $L^*_{100ºC}$ = whiteness-degree of natural samples, $L^*_{900ºC}$ = whiteness-degree at 900 ºC heated samples; $a^*_{100ºC}$, $b^*_{100ºC}$, $a^*_{900ºC}$, $b^*_{900ºC}$ CIELAB color parameters of natural samples and after firing at 900ºC.

Sample	1	2	3	4	5	6	7	10	11	12	13	14	15	16	17	18	19	20	21	22	23	24	25	26	27
PL	12.80	25.63	37.77	34.25	38.92	28.6	27.32	31.96	31.77	36.06	31.33	24.17	38.95	32.66	23.42	31.77	39.77	42.49	27.13	32.81	34.96	24.76	46.44	27.94	56.83
LL	16.86	32.17	54.87	59.14	60.42	51.17	39.58	51.58	53.35	58.82	44.99	30.39	56.23	47.31	27.83	53.51	62.73	64.69	35.58	50.96	61.53	42.87	27.91	41.60	75.10
PI	4.07	6.54	17.10	24.88	21.50	22.57	12.27	19.62	21.58	22.76	13.66	6.22	17.28	14.65	4.41	21.73	22.96	22.20	8.45	18.15	26.57	18.11	18.73	13.66	18.27
BS_d	3	4	16	36	32	25	12	12	36	46	13	5	4	24	10	26	21	44	7	22	52	8	19	30	13
$LS_{w/d}$	5	4	5	12	6	10	8	7	7	9	5	6	5	8	5	9	9	10	5	11	8	8	7	7	11
WA_{900}	26.53	26.54	23.09	15.63	20.32	12.03	16.44	23.62	15.11	14.47	22.39	22.81	28.67	17.69	24.79	13.28	18.88	13.16	22.56	17.37	14.06	9.96	11.98	9.79	18.42
BS_{900}	6	12	112	206	154	69	21	54	170	139	22	20	11	92	14	72	72	194	8	32	168	135	110	247	90
$LS_{d/f}$	1	1	1	1	2	2	1	1	1	1	1	1	1	2	1	2	2	2	1	1	2	1	2	2	5
$LS_{t\ 900}$	6	5	6	10	8	12	9	8	8	10	6	7	6	10	6	11	11	12	6	12	10	9	9	9	16
$L^*_{100ºC}$	61.4	62.9	64.4	71.8	72	82.7	85.1	62.2	72	78.2	65.1	59.7	65.1	76.0	59.6	75.6	68.2	80.7	81.5	79.3	82.9	68.6	75.7	75.1	84.1
$L^*_{900ºC}$	59.1	59.7	53.5	53.4	56.3	65.9	73.4	56.3	57.9	59.6	60.4	58.1	56.9	57.7	55.8	56.6	58.7	58.6	69.9	59.8	70.9	57.6	58.0	58.7	63.6
$a^*_{100ºC}$	25.2	26.0	22.8	7.7	13.5	0.6	1.1	25.3	10.6	1.9	19.9	29.6	24.6	7.7	25.9	2.2	17.4	1.0	1.6	5.6	1.4	17.5	8.6	9.8	0.2
$a^*_{900ºC}$	28.7	30.5	30.7	26.1	26.0	13.9	13.2	31.4	26.2	19.7	27.9	32.5	31.0	24.7	29.8	26.6	27.8	17.7	14.4	24.9	15.1	29.0	29.3	27.5	16.8
$b^*_{100ºC}$	27.2	35.4	30.0	29.5	26.6	6.6	8.6	34.6	28.5	17.4	29.6	35.3	34.0	25.2	31.9	16.7	27.0	14.4	11.5	26.3	10.9	33.2	29.7	31.2	13.4
$b^*_{900ºC}$	26.6	30.9	27.6	27.9	25.2	25.4	26.5	30.4	28.7	27.4	27.8	30.8	31.0	28.3	28.3	29.4	30.1	26.7	23.5	28.5	24.3	28.0	29.6	29.4	28.7

Table 3 (continued)

Sample	28	29	30	31	32	33	34	35	36	37	38	39	40	41	42	43	44	45	46	47	48	49	50	51	52	53
PL	34.37	33.96	47.42	32.84	31.49	24.25	29.98	23.35	34.08	23.65	28.30	15.77	36.62	37.30	28.16	22.99	35.02	34.83	32.16	30.10	30.16	18.38	24.54	35.00	28.03	34.27
LL	51.87	50.64	70.40	49.98	47.59	37.99	45.13	35.84	55.25	32.48	43.73	17.63	52.25	53.66	47.81	29.15	64.26	71.94	54.19	46.84	47.4	23.96	31.86	49.97	47.06	56.33
PI	17.50	16.68	22.97	17.14	16.10	13.74	15.15	12.49	21.17	8.83	15.43	1.85	15.63	16.35	19.64	6.17	29.24	37.11	22.02	16.74	17.24	5.58	7.33	14.98	19.04	22.06
BS_d	27	27	29	19	4	10	21	14	27	14	22	6	24	13	34	3	25	26	10	26	11	3	2	55	16	23
$LS_{w/d}$	5	5	12	10	5	5	7	6	4	8	7	4	10	8	7	5	10	9	6	8	7	2	3	4	6	10
WA_{900}	14.92	15.63	13.40	16.39	23.85	16.50	10.25	15.14	19.28	19.19	11.96	19.51	18.80	18.81	8.11	19.84	12.09	13.30	16.20	14.20	14.40	18.10	21.32	17.01	18.60	12.50
BS_{900}	118	161	140	53	7	50	117	34	52	22	116	16	25	87	198	4	134	271	140	112	94	14	4	86	38	57
$LS_{d/f}$	5	4	4	1	1	1	3	2	5	1	2	1	2	2	3	1	5	6	6	3	2	0	2	1	1	1
$LS_{t\ 900}$	10	9	16	11	6	6	10	8	9	9	9	5	12	10	10	6	15	15	12	11	9	2	5	5	7	11
$L^*_{100ºC}$	75.4	76.6	85.5	80.4	71.0	70.6	73.2	82.4	76.8	75.2	73.6	78.4	72.5	81.0	79.1	49.0	75.9	78.8	80.6	73.4	78.5	72.5	86.8	85.6	74.0	76.6
$L^*_{900ºC}$	55.2	60.5	49.8	59.2	63.8	58.9	56.5	59.5	61.1	60.3	57.0	66.1	62.8	57.5	56.2	56.0	58.7	49.4	53.4	57.8	56.9	75.8	82.9	63.9	75.3	63.4
$a^*_{100ºC}$	7.0	6.7	0.4	4.0	14.3	11.7	4.0	0.2	4.4	3.1	3.8	0.1	11.3	3.4	6.4	32.6	10.9	4.0	3.6	8.0	3.0	2.7	1.3	2.2	3.2	8.1
$a^*_{900ºC}$	28.4	27.5	19.8	23.4	21.2	26.6	23.2	16.9	24.2	18.3	21.7	21.7	20.2	20.4	26.8	30.4	24.6	26.5	27.4	29.3	25.8	9.8	8.0	16.3	11.6	18.0
$b^*_{100ºC}$	26.7	27.1	13.3	22.5	20.9	28.3	20.8	8.3	23.1	16.6	19.7	9.9	18.9	22.2	29.3	32.4	19.9	20.5	21.7	28.4	21.2	6.1	11.4	10.6	11.8	16.7
$b^*_{900ºC}$	30.3	31.6	26.2	28.6	24.4	26.6	27.5	28.2	28.6	26.0	27.6	25.4	26.0	26.7	26.4	30.2	28.0	25.7	28.2	31.1	26.8	15.9	14.9	27.8	17.8	27.3

Table 4. Descriptive statistics for the 41 variables and 51 sample distributions. The abbreviations are: Ilt = illite; Kln = kaolinite, Qz = quartz; Fsp = feldspar; ML+Sme+Chl = interstratified clay minerals, smectite, and chlorite; PL = plastic limit; LL = liquid limit; PI = plasticity index; $pH_{1'}$ = after 1 min; $pH_{15'}$ = after 15 min; WA_{900} = water absorption 900ºC; BS_d = dry bending strength; BS_{900} = fired bending strength 900ºC; $LS_{w/d}$ = wet/dry linear shrinkage; $LS_{d/f}$ = dry/fired linear shrinkage; $LS_{t\ 900}$ = total linear shrinkage 900ºC; clay m. = clay minerals; n.clay m. = non-clay minerals; (t) = total sample, (c) = <2μm fraction; and ND = not determined (zero values in the dataset).

	Mean	G. Mean	Median	Minimum	Maximum	Std-Dev.	Coef. Var.	Skewness	Kurtosis
SiO_2	64.64	64.20	63.76	49.79	84.52	7.63	0.12	0.33	0.18
Al_2O_3	16.90	16.53	17.19	8.08	23.73	3.45	0.20	−0.17	0.15
Fe_{tot}	5.16	4.68	5.81	0.95	8.05	1.89	0.37	−0.76	−0.64
MgO	1.19	0.89	0.99	0.09	5.32	0.90	0.76	2.23	8.26
K_2O	3.13	2.96	3.10	0.73	5.27	0.93	0.30	−0.08	1.01
TiO_2	0.77	0.72	0.81	0.10	1.25	0.23	0.30	−0.57	0.36
LOI	7.39	7.03	7.35	2.63	13.33	2.24	0.30	0.32	0.68
$Ilt_{(t)}$	30.45	25.55	33.00	3.00	61.00	13.86	0.46	−0.39	−0.28
$Kln_{(t)}$	14.80	ND	13.00	0.00	37.00	9.20	0.62	0.56	−0.56
$Qz_{(t)}$	37.76	35.31	38.00	14.00	74.00	13.99	0.37	0.73	0.16
$Ilt_{(c)}$	40.33	36.49	40.00	7.00	72.00	15.56	0.39	−0.11	−0.15
$Kln_{(c)}$	33.69	27.58	28.00	1.00	90.00	19.53	0.58	0.85	0.34
$Qz_{(c)}$	6.39	4.60	5.00	1.00	22.00	5.38	0.84	1.44	1.47
<2μm	13.28	11.50	10.49	2.25	37.20	7.42	0.56	1.28	1.39
2−63μm	71.63	68.46	76.71	10.83	88.05	16.63	0.23	−1.81	3.14
>63μm	15.45	6.96	7.85	0.03	84.00	19.07	1.23	1.98	3.43
L^*_{100}	74.38	73.94	75.60	49.00	86.80	7.86	0.11	−0.90	0.98
a^*_{100}	9.18	4.82	6.40	0.10	32.60	8.97	0.98	1.12	0.12
b^*_{100}	22.02	20.09	22.20	6.10	35.40	8.44	0.38	−0.23	−1.08
L^*_{900}	60.28	59.97	58.70	49.40	82.90	6.45	0.11	1.50	2.83
a^*_{900}	23.32	22.34	24.90	8.00	32.50	6.17	0.26	−0.68	−0.42
b^*_{900}	27.15	26.90	27.80	14.90	31.60	3.35	0.12	−2.05	5.43
$pH_{1'}$	6.28	6.17	6.00	4.27	8.61	1.23	0.20	0.44	−0.99
$pH_{15'}$	6.16	6.03	5.84	4.26	8.58	1.28	0.21	0.53	−1.09
PL	31.52	30.55	31.77	12.80	56.83	7.74	0.25	0.46	1.83
LL	47.38	45.21	49.97	16.86	75.10	13.30	0.28	−0.31	−0.14
PI	16.59	14.69	17.14	1.85	37.11	6.89	0.42	0.04	0.68
WA_{900}	17.14	16.42	16.50	7.09	28.67	4.88	0.35	0.25	−0.27
BS_d	19.82	15.15	19.00	2.00	55.00	12.92	0.65	0.76	0.34
BS_{900}	85.88	53.70	72.00	4.00	271.00	68.43	0.80	0.73	−0.11
$LS_{w/d}$	7.06	6.63	7.00	2.00	12.00	2.39	0.34	0.21	−0.64
$LS_{d/f}$	2.10	ND	2.00	0.00	6.00	1.51	0.72	1.30	0.68
$LS_{t\ 900}$	9.16	8.59	9.00	2.00	16.00	3.09	0.34	0.24	−0.16
$Fsp_{(t)}$	8.16	ND	4.00	0.00	38.00	8.54	1.05	1.73	2.72
clay $m._{(t)}$	52.75	48.61	54.00	8.00	85.00	17.18	0.33	−0.74	0.37
n.clay $m._{(t)}$	47.24	44.25	46.00	15.00	92.00	17.15	0.36	0.74	0.39
$ML+Sme+Chl_{(t)}$	7.51	ND	5.00	0.00	30.00	7.23	0.96	0.87	0.30
clay $m._{(c)}$	91.92	91.62	95.00	72.00	99.00	7.23	0.08	−1.56	1.69
n.clay $m._{(c)}$	7.55	5.59	6.00	1.00	27.00	6.22	0.82	1.54	1.99
$ML+Sme+Chl_{(c)}$	18.29	ND	16.00	0.00	57.00	16.47	0.90	0.62	−0.36

of the positive correlations were diminished. The positive correlation between LOI and BS_{900}, $LS_{t\ 900}$, and PI indicated a strong relationship between these ceramic properties and the clay mineral contents (Table 5). Significant correlations between ceramic properties indicate the expected interdependence of these properties. Correlations between the variables examined in the present study were usually not strong and reflected the compositional heterogeneity of the samples and the complexity of the variables, which were often mutually dependent and dependent on variables that were not considered in the system.

Factor analysis. According to the results of R-mode FA applied to the full data set (12 × 51, Table 6), the principal component analysis (Kaiser, 1958; Cattell, 1966) extracted four factors, which explained a total variance of 84.4%. Varimax normalized factor rotation resulted in a better contrast between the maxima and minima loadings and increased the interpretability. Communalities were higher than 0.75, except for the <2 μm variable. A communality value of 0.7 is the lower limit for credible results using FA (Castaing, 1973); hence, the four-factor model explained the variability of almost all the variables and can be used to indicate

https://doi.org/10.1346/CCMN.2016.064040 Published online by Cambridge University Press

Table 5. Spearman rank coefficients of the sample (n = 51) variables at p <0.05 and the most significant correlations for r ⩾ |0.6| in bold print.

	SiO_2	Al_2O_3	Fe_{tot}	MgO	K_2O	TiO_2	LOI	$Ilt_{(t)}$	$Kln_{(t)}$	$Qz_{(t)}$	$Ilt_{(c)}$	<2µm	>63µm	L^*_{100}	b^*_{100}	a^*_{900}	PI	Ab_{900}	BS_d	BS_{900}	$LS_{t\ 900}$	$Fsp_{(t)}$	clay $m._{(t)}$	ML+Sme+$Chl_{(t)}$
SiO_2	1.00																							
Al_2O_3	**−0.80**	1.00																						
Fe_{tot}	**−0.80**	0.73	1.00																					
MgO	**−0.60**	0.15*	0.39	1.00																				
K_2O	−0.52	0.35	0.30	0.52	1.00																			
TiO_2	−0.16*	0.35	0.41	−0.08*	−0.32	1.00																		
LOI	**−0.82**	0.53	0.54	0.57	0.35	−0.06*	1.00																	
$Ilt_{(t)}$	**−0.69**	0.69	0.65	0.41	0.44	0.31	0.47	1.00																
$Kln_{(t)}$	−0.08*	0.46	0.20*	−0.54	−0.20*	0.28	0.03*	0.18*	1.00															
$Qz_{(t)}$	**0.76**	−0.65	−0.49	−0.51	**−0.64**	−0.07*	**−0.62**	−0.77	−0.12*	1.00														
$Ilt_{(c)}$	**−0.61**	0.57	**0.72**	0.38	0.30	0.37	0.35	**0.80**	0.05*	−0.49	1.00													
<2µm	−0.47	0.48	0.55	0.13*	0.10*	0.17*	0.44	0.46	0.37	−0.22*	**0.61**	1.00												
>63µm	**0.83**	−0.67	−0.72	−0.52	−0.33	−0.28	−0.70	−0.74	−0.10*	**0.60**	−0.71	−0.64	1.00											
L^*_{100}	−0.09*	−0.19*	−0.28	0.31	0.37	**−0.66**	0.30	−0.01*	−0.24*	−0.16*	0.15*	0.12*	−0.12*	1.00										
b^*_{100}	−0.18*	0.31	0.59	−0.02	−0.30	**0.79**	−0.08*	0.32	0.24*	−0.01*	0.53	0.25*	−0.28	**−0.73**	1.00									
a^*_{900}	−0.22*	0.36	**0.61**	−0.02*	−0.15*	**0.72**	−0.07*	0.33	0.27*	−0.07*	0.54	0.27*	−0.27*	**−0.71**	0.92	1.00								
PI	**−0.62**	0.42	0.44	0.41	0.24*	−0.04*	**0.79**	0.37	0.15*	−0.42	0.33	0.40	−0.55	0.27*	−0.08*	−0.07*	1.00							
Ab_{900}	0.40	−0.08*	−0.21*	−0.57	−0.38	0.39	−0.51	−0.08*	0.16*	0.23*	0.16*	−0.40	0.31	−0.44	0.24*	0.18*	−0.54	1.00						
BS_d	−0.39	0.26	0.17*	0.32	0.30	−0.02*	0.51	0.14*	−0.19*	−0.37	−0.06*	0.04*	−0.36	0.42	−0.17*	−0.12*	0.61	−0.54	1.00					
BS_{900}	**−0.74**	0.39	0.58	**0.70**	0.48	−0.06*	**0.74**	0.44	−0.13*	−0.51	0.38	0.38	**−0.61**	0.24*	0.06*	0.06*	**0.69**	−0.74	0.78	1.00				
$LS_{t\ 900}$	−0.53	0.20*	0.35	0.54	0.25*	−0.13*	**0.71**	0.30	−0.13*	−0.31	0.34	0.48	−0.53	0.35	−0.12*	−0.10*	**0.72**	−0.67	0.56	**0.61**	1.00			
$Fsp_{(t)}$	0.09*	−0.39	−0.31	0.37	0.46	−0.52	−0.02*	0.32	**−0.70**	−0.02*	0.29	−0.44	0.29	0.37	−0.54	−0.47	−0.02*	−0.28	0.32	0.16*	0.15*	1.00		
clay $m._{(t)}$	**−0.73**	0.73	0.59	0.36	0.35	0.28	**0.60**	0.88	0.37	−0.86	0.62	0.42	**−0.73**	0.02*	0.22*	0.25*	0.48	−0.10*	0.28	0.43	0.33	−0.36	1.00	
ML+Sme+$Chl_{(t)}$	−0.23*	−0.22*	−0.01*	**0.70**	0.23*	−0.10*	0.39	−0.02*	**−0.65**	−0.25*	0.06*	−0.18*	−0.22*	0.35	−0.16*	−0.22*	0.31	−0.38	**0.65**	0.47	0.39	0.52	0.03*	1.00

* Non significant correlations, p <0.05

Table 6. Varimax normalized and unrotated (in brackets) factor loadings, communalities, eigenvalues, and the explained values of the variance.

	Factor Loadings (Varimax normalized) — Extraction: Principal Components (Loadings marked in bold print are >0.700)								
	Factor 1		Factor 2		Factor 3		Factor 4		Communalities
Al_2O_3	**0.751**	(−0.901)	−0.150	(−0.227)	0.369	(0.141)	−0.412	(−0.104)	0.893
$Fe_{(t)}$	**0.877**	(−0.806)	0.146	(−0.105)	0.214	−0.012)	0.026	0.418)	0.837
K_2O	0.404	(−0.500)	**−0.866**	(0.403)	0.145	(0.688)	0.020	−0.225)	0.935
LOI	0.504	**(−0.826)**	0.019	(0.219)	**0.767**	(−0.324)	0.004	(−0.090)	0.844
$Ilt_{(t)}$	**0.951**	(−0.840)	−0.081	(−0.142)	0.088	(0.265)	−0.074	(0.356)	0.924
$Kln_{(t)}$	0.129	(−0.275)	0.164	**(−0.755)**	0.061	−0.037)	**−0.880**	(−0.417)	0.821
$Qz_{(t)}$	**−0.782**	(0.851)	0.398	(−0.178)	−0.315	−0.328)	0.001	(−0.075)	0.869
<2μm	0.466	(−0.659)	0.028	(−0.299)	0.370	(−0.066)	−0.461	−0.199)	0.567
PI	0.277	**(−0.724)**	0.002	(0.235)	**0.883**	(−0.426)	−0.093	(−0.322)	0.865
BS_d	0.016	(−0.424)	−0.222	(0.636)	**0.796**	(−0.310)	0.281	(−0.286)	0.762
$Fsp_{(t)}$	−0.499	(0.399)	**−0.728**	(0.706)	−0.016	(0.402)	0.383	(−0.326)	0.926
ML+Sme+$Chl_{(t)}$	0.085	(−0.148)	−0.024	**(0.816)**	0.411	(−0.282)	**0.842**	(0.344)	0.886
Eigenvalues	5.219	2.607	1.300	1.000					
Explained Var	43.489	21.727	10.836	8.347					
Cum Eigenv	5.219	7.826	9.126	10.128					
Cum Var (%)	43.489	65.217	76.053	84.399					

which variables to retain. Factor 1 explained 43.49% of the total variance, had a high eigenvalue (5.22), and indicated a good response of individual factors towards defining the significant relationships and processes. Factor 1 reflected the association between alumina and illite, which was the most common clay mineral in the sample ensemble. Factor 1 also reflected the chroma and particularly the Fe, which correlated with the reddish hues. The highest factor 1 scores reflected the red structural clays (*e.g.* samples 5, 46, and 48) in contrast to the raw materials with generally lighter colors and negative factor 1 scores, which can be used for blending with plastic clays (*e.g.* samples 7, 35, and 49; Figure 5a). Higher positive factor 1 scores usually represented the illitic clays with higher ceramic quality in terms of technological properties. Factor 2 described 21.73% of the variance and grouped the K_2O and feldspars. Negative factor 2 scores indicated samples with higher feldspar contents and samples with greater illite contents (*e.g.* samples 39, 46, and 51). In contrast, samples rich in clay minerals other than illite or rich in quartz had positive factor 2 scores (*e.g.* samples 43 and 53; Figure 5b). Factor 3 explained 10.84% of total variance and reflected the ceramic properties of clay minerals (strong positive loadings on PI, BS_d, and LOI). The highest positive factor 2 scores were for clay-rich samples and/or samples enriched in smectite or interstratified clay minerals and indicated the samples of higher ceramic quality (*e.g.* samples 23 and 45). Those samples that lacked plasticity and strength (low clay mineral content) had the lowest negative factor 3 scores, namely, the Campelo Formation samples in Tábua (*e.g.* samples 1, 2, and 17) and the feldspar-rich samples (*e.g.* sample 39; Figure 5c). Factor 4 accounted for only 8.35% of the total variance and stressed the opposite relationship between kaolinite and 14 Å clay minerals (smectite, chlorite, and interstratified clay minerals). The factor 4 scores indicate a distinction between kaolinitic samples (higher negative factor scores) and samples with smectite, chlorite, and interstratified clay minerals (higher positive factor scores; Figure 5d).

Cluster Analysis. Despite the possible redundancy, mineralogical and ceramic variables were considered together with chemical variables for hierarchical CA and the resulting dendogram (Figure 6). This procedure resulted in a better discrimination between the clusters of samples, in addition to an enhancement of the variance explained by factor analysis. Two main assemblages of variables were joined at the linkage distance of approximately 2.9. A major assemblage group A (GA) evidenced the relationship between clay minerals, chemical variables, particle size, and plasticity. On a higher level of similarity, this group may be subdivided into three sub-groups that reflect the affinity between Fe and illite (A1), the plasticity of clay minerals (A2), and kaolinite only (A3), which was related to clay minerals in general. The other assemblage (group B, GB) grouped non-clay minerals and 14 Å clay minerals. On a higher level of similarity, this group may also be subdivided into three sub-groups that reflect the feldspar content in a significant number of samples (B1), the smectite clay mineral relationship with bending strength (B2), and quartz (B3). This is in contrast to clay minerals and related variables, which were indicated by factor 1 in R-mode FA. The data were analyzed in Q-mode in

https://doi.org/10.1346/CCMN.2016.064040 Published online by Cambridge University Press

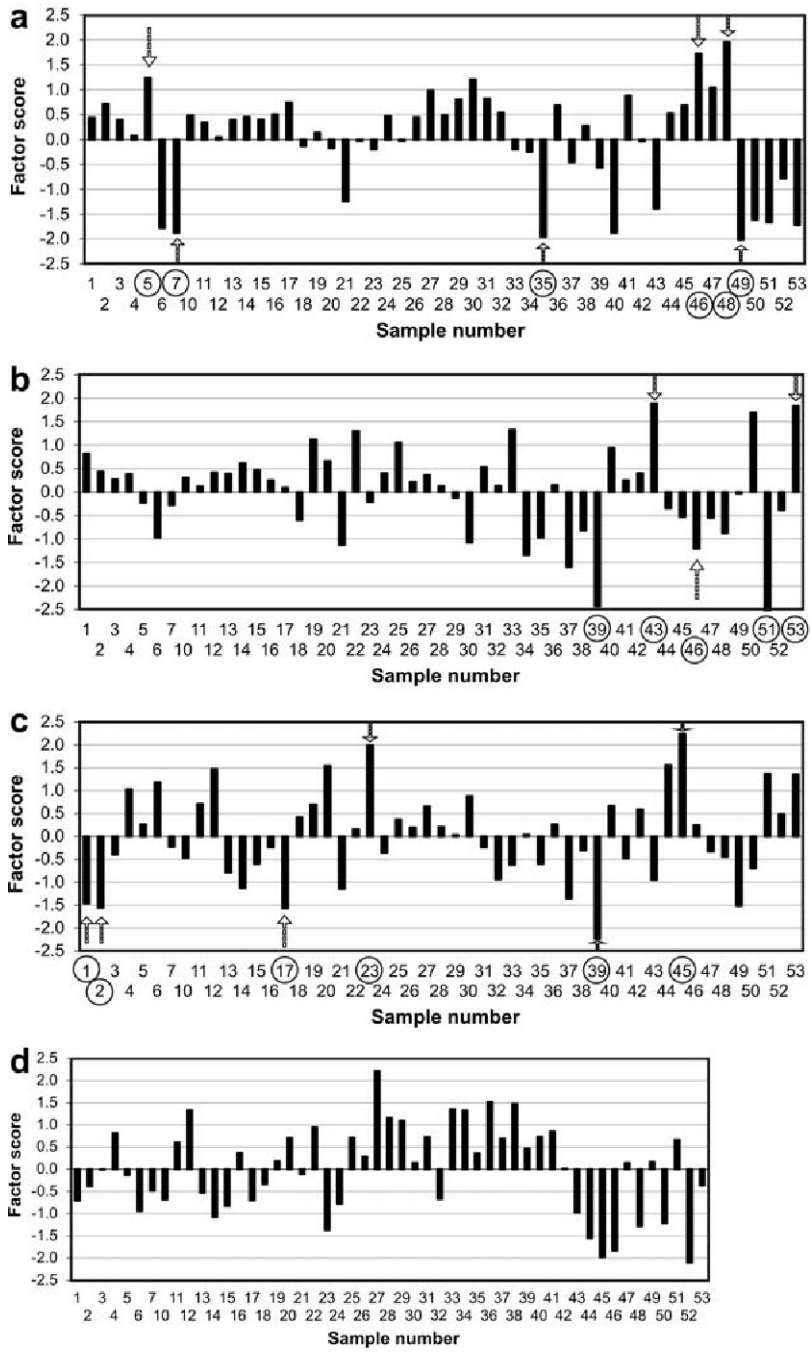

Figure 5. Factor analysis (FA) scores of the 51 samples: (a) Factor 1, (b) Factor 2, (c) Factor 3, and (d) Factor 4.

order to highlight similarities between samples. The CA classified the samples in two main groups (Figure 7): clayey-silt samples and sandy and/or feldspathic samples (non-clay minerals were dominant). The cluster of clayey-silt samples was in turn subdivided into sub-clusters *I* and *II*. The sub-cluster *I* was characterized by samples that contained kaolinite with minor amounts or no smectite, interstratified clay minerals, and chlorite. On a higher level of similarity, this group may also be subdivided into two sub-groups and both revealed a high similarity between samples. Sub-group *Ia* samples belong to the Campelo Formation in the Tábua region, with the exception of samples 24, 32, and 52, which belong to the Buçaqueiro Formation. Apart from sample 52, all the samples encompassed upper layers of the Campelo Formation infilling. Sub-group *Ib* samples

https://doi.org/10.1346/CCMN.2016.064040 Published online by Cambridge University Press

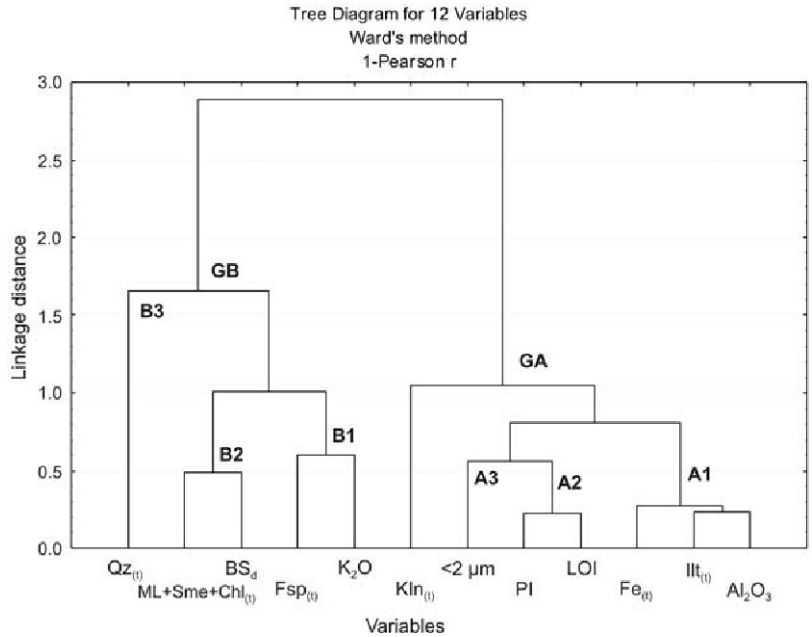

Figure 6. Tree diagram produced by Cluster Analysis (CA) of variables in the composition of ceramic raw materials.

belong to the Campelo Formation and were collected in the same area (Miranda do Corvo region) and stratigraphic level. Sample 47 (sub-cluster *II*) was collected in this area, but it belongs to a lower stratigraphic column position. At a higher linkage distance from sub-cluster *I*, the sub-cluster *II* comprised the largest number of samples rendered in common with the presence of 14 Å clay minerals. Samples 27, 28, 29, and 30 were linked at a low similarity level to samples 25 and 26 and were considered to belong to the Coja and Campelo formations, respectively, in the Santa Quitéria region. The strong correlation between samples 36 and 38 (Coja region) and samples collected in the Coja Formation in Santa Quitéria was also noticeable. The samples inferred

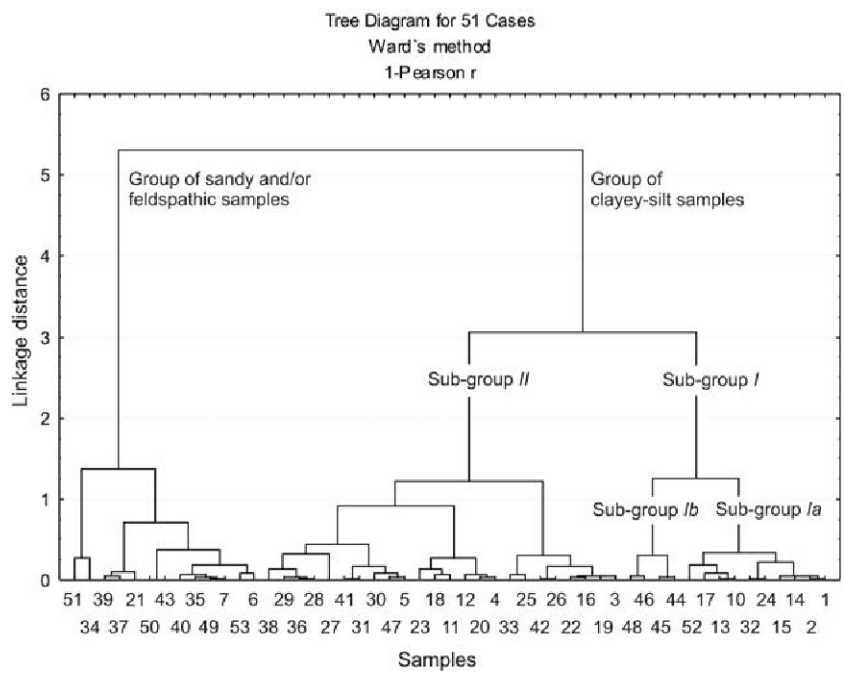

Figure 7. Tree diagram produced by Cluster Analysis (CA) of the 51 samples of ceramic raw materials.

https://doi.org/10.1346/CCMN.2016.064040 Published online by Cambridge University Press

to the Coja Formation in Tábua were also included in this sub-group, but the degree of similarity between these and the rest of the samples were more difficult to assess. Sub-group *II* encompassed samples of the upper member of the Coja Formation and of the Sacões Group. The group of sandy and/or feldspathic samples represented sediments that were either arenitic or had a low clay mineral content and a significant content of feldspars, which stratigraphically belonged to the Buçaco Group formations, the lower member of the Coja Formation, or even encompassed remobilized sediments from the Coja Formation in the Campelo Formation.

Samples 34 and 51 both had a high similarity, but differed from all other samples of the group in which the sand fraction was higher. The clusters through different combinations of variables did not differ significantly and certain groups remained regardless of the different combinations. The stability of these groups enhanced the relative confidence in the results.

DISCUSSION

The suitability of raw clays for use in the manufacture of ceramic products is determined by the physical properties, mineralogy, and chemistry of the material. These factors will determine the behavior of the clay during all phases of the manufacturing process with a direct influence on the final product. The analytical results showed that the particle size of the samples was dominantly silt and was frequently deficient in sand, especially clay, and was suitable for direct use in tile or brickmaking. The significant amounts of feldspar and more often quartz indicated poor technological properties, such as low plasticity and bending strength (dry and fired), which were the most obviously affected properties (Table 3). Other factors or minerals can reduce the influence of quartz and feldspar minerals and improve the technological properties, such as expandable clay minerals. Additionally, most samples required slow ceramic firing in the 500−600ºC range to avoid sudden quartz expansion. The balance of clay minerals in the samples was frequently satisfactory, but clays with higher contents of smectite or mixed-layer smectite/chlorite require special attention during drying. The chemical composition of the samples was deficient in CaO and reflects the absence of calcite/dolomite. According to the factor model, among the 12 variables selected, the variables which most contributed to the sample groupings were Al_2O_3, Fe_{tot}, $Ilt_{(t)}$, $Qz_{(t)}$, $Fsp_{(t)}$, and K_2O and other variables had a more discrete role. The R-mode CA statistical techniques substantiated these results for the relationships between variables. Both the R-mode FA and CA techniques identified a strong relationship between Al_2O_3, Fe_{tot}, and illite contents in contrast to quartz and feldspar contents. An inverse relationship was found between kaolinite and expandable clay mineral contents. The interpretation of the bending strength relationships was slightly different for the statistical analyses using R-mode FA and CA. The FA indicated high positive factor loadings (>0.7) for bending strength, plasticity index, and LOI (factor 3), but in CA the bending strength had a smaller linkage distance with expandable clay minerals. This slight divergence was apparent because the variables involved were closely interrelated, as the similar Spearman rank coefficient values indicated (Table 4). The statistical analysis allowed a limited set of parameters to be selected to characterize the raw materials. This can be used to first separate the open-stockpile materials (preferably in the pit), which can later be blended into the desired and distinct ceramic product compositions. The Q-mode CA allowed the samples to be consistently grouped to discriminate between lithological and mineralogical attributes and also permitted the stratigraphic relationships to be inferred and, hence, to relate the clusters to the suitability of the corresponding raw materials for the manufacture of ceramic bodies. Diagrams that relate grain size and chemistry parameters to the ceramic suitability of the materials (Figures 8 and 9) and the reference values for ceramic blends that are used in the manufacture of common ceramic products (Table 7) support the clusters generated by the statistics. The samples of sub-group Ia generally matched clays with a low ceramic propensity, which need to be adequately blended with plastic clays (Table 2) to improve the plasticity and the bending strength (both dry and fired) and to diminish water absorption for the manufacture of brick, vaulted brick, and masonry. The Winkler diagram (Winkler, 1954) indicated that the samples from sub-group Ia (apart from samples 14 and 24) and from sub-group Ib require the addition of clay and sand, respectively. The latter sub-group of samples showed the best properties for building bricks and require the addition of sand (quartz and feldspar), especially for the manufacture of tile and accessories in order to prevent the excessive shrinkage that is observed (Tables 3 and 7). The ceramic suitability of clayey materials from sub-group II was variable and most samples required modification of the initial composition and required blending with clay and sand (Figure 8). Additionally, the heating process must be conducted with precaution by creating a low-heating rate stage on drying up to 200ºC due to the presence of smectitic clay minerals. Raw materials that encompassed the group of sandy and/or feldspathic samples were both poor in clay and silt (Figure 8) and most had low BS_{900} and PI values. Such materials can be used for blending with low sand content samples and with excessively plastic clays with high PI (44 and 45) or PL (*e.g.* samples 20, 25, 30, 27) and were reflected by the high shrinkage values (Bain and Highley, 1979; Table 3). The chemical data were plotted on a ternary diagram (silica-alumina-other oxides) to classify clay raw materials and industrial ceramic bodies (Fabbri and Fiori, 1985; Figure 9). The diagram shows that most samples fitted into the Portuguese red stoneware field (Lisboa,

https://doi.org/10.1346/CCMN.2016.064040 Published online by Cambridge University Press

Table 7. Reference values for the ceramic blends used in the manufacture of common ceramic products and the mineralogical composition types for hollow brick manufacture (Fabbri and Dondi, 1995; Martins, 2007); (a) values from Strazzera *et al.* (1997); (b) values from Santos (1975); and (–) value not available.

Parameters	Brick	Vaulted brick	Tile	Mineral	(%)
BS_d (kg/cm^2)	45–50	50–60	70–90	Quartz	3–40
BS_d (kg/cm^2) [(a)]	15–51	–	20–51	Illite/mica	2–30
BS_d (kg/cm^2) [(b)]	>15	–	>30	Calcite/Dolomite	0–25
$LS_{w/d}$ (max. value, %)	5	5	6	Chlorite	0–10
$LS_{w/d}$ (%) [(a)]	3–12	–	3–8	Kaolinite	0–15
Drying cycle (h)	24–48	24–36	48	Smectite	0–20
				Feldspar	5–10
Firing temp. (ºC)	900 ± 50	900 ± 50	1000 ± 50	Fe oxides, hydroxides	5–10
BS (kg/cm^2)	⩾100	⩾130	⩾160		
BS (kg/cm^2) [(a)]	61–143	122–204	122–224		
BS (kg/cm^2) [(b)]	>55	–	>65		
LS_t (%)	5–6	5–6	5–6		
WA (%)	10–17	10–17	10 (max.)		
WA (%) [(a)]	15–32	–	15–20		

2014) apart from sub-group Ib and the sandy and/or feldspathic samples. The former samples were more enriched in clay minerals and contained less quartz than average Portuguese red ceramic bodies. The majority of the latter group plotted in the range between the white stoneware and the quartz/feldspathic sands field.

CONCLUSION

Based on an assessment of the compositional and technological data of 51 argillaceous samples, factor analysis and cluster analysis were shown to be a powerful tool in interpreting the ceramic types of raw materials and also were an aid in differentiating the stratigraphy of layers. Among the 41 mineralogical, chemical, and technological variables, 12 variables were selected based on a closer proximity to normal distributions. From those variables based on R-mode FA and CA, the variables which contributed most to the sample groupings were Al_2O_3, Fe_{tot}, $Ilt_{(t)}$, $Qz_{(t)}$, $Fsp_{(t)}$, and K_2O. The cluster analysis results were substantiated by the ceramic suitability diagrams, which assigned most

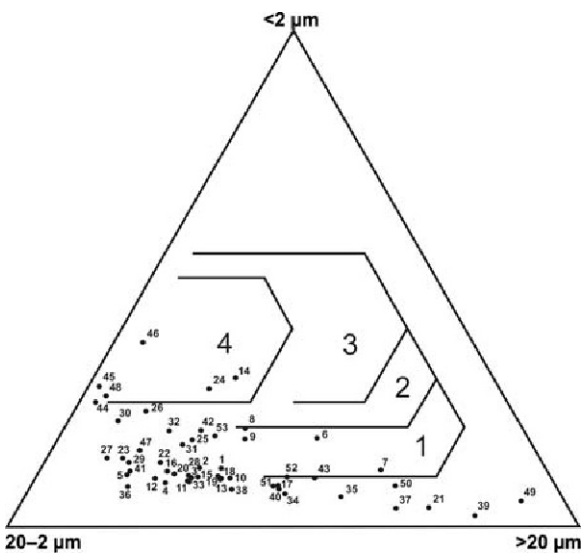

Figure 8. Winkler diagram (Winkler, 1954) for the technical classification of ceramic raw materials for use in structural clay products. The fields indicate compositions suitable for 1- solid bricks, 2- vertically perforated bricks, 3- roofing tiles, and 4- thin-walled hollow bricks.

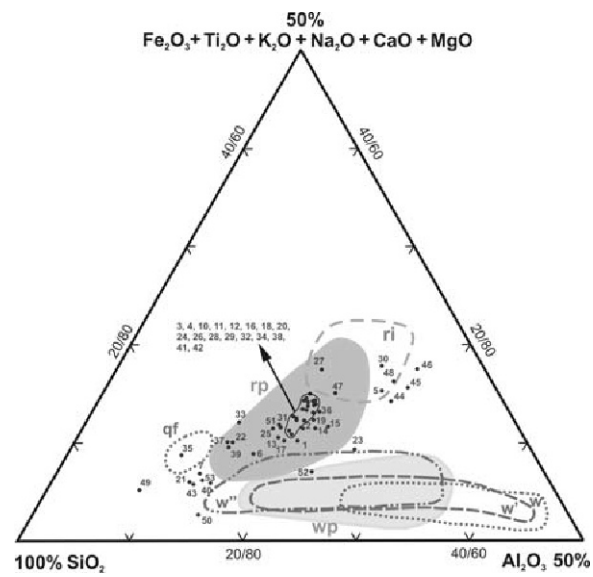

Figure 9. Ternary diagram for SiO_2/Al_2O_3/ Fe_2O_3+TiO_2+ MgO+K_2O+Na_2O composition with plotted samples of the clay raw materials where ri = red stoneware (Italy); qf = quartz/ feldspathic sands field; w, w′, and w″ = white stoneware for the German, English, and French industries, respectively (data from Fabbri and Fiori, 1985); and rp and wp refer to Portuguese 'red' and 'white' ceramics, respectively (data from Lisboa, 2014).

https://doi.org/10.1346/CCMN.2016.064040 Published online by Cambridge University Press

samples to red stoneware, which is suitable for brick and tile manufacture after adequate blending. The majority of the sampled raw materials were rich in silt and required the addition of sand and/or clay. Due to the high quartz and/or expansive clay mineral content of some of the sampled materials, special attention is required for firing and drying.

Apart from the recognized practical usefulness of diagrams that relate specific parameters with the suitability of materials for ceramics, the diagrams rely on a very limited number of variables. Multivariate analysis and particularly CA produced an interpretation based on multiple variables and, therefore, improved interpretation of the ceramic suitability of the material. The groups and sub-groups that resulted from CA have stratigraphical meaning: the group of sandy and/or feldspathic samples encompass arkosic units that belong to the Coja Formation lower member, Buçaqueiro Formation, and Buçaco Group; in the clayey-silt group of samples, sub-group I encompassed the Campelo Formation samples and the sub-group II samples belonged to both the Campelo Formation and Coja Formation upper member. Additionally, within formations, groups can be discriminated by stratigraphic position in the basin infill. The methodology and statistical techniques applied herein can, therefore, be useful in the assessment of clay deposits elsewhere, in which a typological distinction may be a valuable tool to discriminate clay bodies with apparently similar characteristics.

ACKNOWLEDGMENTS

The authors acknowledge the revisions carried out by the editorial staff of the journal as well as three independent reviewers. Their suggestions and comments have greatly improved the quality of the manuscript.

REFERENCES

Agha, M., Ferrell, R.E., and Hart, G.F. (2012) Mineralogy of Egyptian bentonitic clays I: discriminant function analysis. *Clays and Clay Minerals*, **60**, 387–404.

ASTM C 326-82 (1997) *Standard Test Method for Drying and Firing Shrinkages of Ceramic Whiteware Clays*. American Society for Testing and Materials, ASTM International, West Conshohocken, Pennsylvania, USA.

ASTM C 371-09 (2014) *Standard Test Method for Wire-cloth Sieve Analysis of Nonplastic Ceramic Powders*. American Society for Testing and Materials, ASTM International, West Conshohocken, Pennsylvania, USA.

ASTM C 373–88 (1999) *Water Absorption, Bulk Density, Apparent Porosity, and Apparent Specific Gravity of Fired Whiteware Products*. American Society for Testing and Materials, ASTM International, West Conshohocken, Pennsylvania, USA.

ASTM C 674-89 (1999) *Standard Test Methods for Flexural Properties of Ceramic Whiteware Material*. American Society for Testing and Materials, ASTM International, West Conshohocken, Pennsylvania, USA.

ASTM C 689-93 (1997) *Standard Test Method for Modulus of Rupture of Unfired Clays*. American Society for Testing and Materials, ASTM International, West Conshohocken, Pennsylvania, USA.

ASTM D 4318-10 (2010) *Standard Test Methods for Liquid Limit, Plastic Limit, and Plasticity Index of Soils*. American Society for Testing and Materials, ASTM International, West Conshohocken, Pennsylvania, USA.

ASTM D 4972-13 (2013) *Standard Test Method for pH of Soils*. American Society for Testing and Materials, ASTM International, West Conshohocken, Pennsylvania, USA.

Bain, J.A. and Highley, D.E. (1979) Regional appraisal of clay resources – a challenge to the clay mineralogist. In Proceedings of the 6th International Clay Conference, July 1978. (M.M. Mortland and V.C. Farmer, editors). *Developments in Sedimentology*, **27**, 437–446.

Blazek, A. (1972) *Thermal Analysis*. Van Nostrand Reinhold Company, London.

Braekmans, D., Degryse, P., Poblome, J., Neyta, B., Vyncke, K., and Waelkens, M. (2011) Understanding ceramic variability: an archaeometrical interpretation of the Classical and Hellenistic ceramics at Düzen Tepe and Sagalassos (Southwest Turkey). *Journal of Archaeological Science*, **38**, 2101–2115.

Brindley, G.W. and Brown, G. (1980) *Crystal Structures of Clay Minerals and Their X-ray Identification*. Monograph **5**, Mineralogical Society, London.

Bruguera, J. (1985) *Manual Práctico de Cerámica*. Omega, DL, XVI, Barcelona.

Bundy, W.M., Johns, W.D., and Murray, H.H. (1966) Interrelationships of physical and chemical properties of kaolinites. *Clays and Clay Minerals*, **14**, 331–346.

Caputo, H.P. (1998) *Mecânica dos Solos e Suas Aplicações*. Vol.1 and 2, 6th ed. Livros Técnicos e Científicos, Editora S.A., Rio de Janeiro.

Castaing, P. (1973) Remarques sur l'utilisation de l'analyse factorielle en sedimentologie. *Bulletin de l'Institut de Géologie du Bassin d'Aquitaine*, **13**, 53–85.

Cattell, R.B. (1966) The scree-test for the number of factors. *Multivariate Behaviour Research*, **1**, 245–276.

Child, D. (1970) *The Essentials of Factor Analysis*. Holt, Rinehart and Winston, London.

CIE (1978) CIE, Recommendations on Uniform Color Space, Color-difference Equations and Psychometric Color Terms. Supplement 2 to CIE Publication 15, Commission Internationale de l'Eclairage, Paris.

Cravero, F., Marfil, S.A., and Maiza, P.J. (2010) Statistical analysis of geochemical data: a tool for discriminating between kaolin deposits of hypogene and supergene origin, Patagonia, Argentina. *Clay Minerals*, **45**, 183–196.

Cunha, P.R.P. (1992) *Estratigrafia e Sedimentologia dos Depósitos do Cretácico Superior e Terciário de Portugal Central, a leste de Coimbra*. PhD thesis, Univ. Coimbra, Coimbra, Portugal, 263 pp.

Cunha, P.R.P. (1999) Unidades litostratigráficas do Terciário na região de Miranda do Corvo-Viseu (Bacia do Mondego, Portugal). *Comunicações do Instituto Geológico e Mineiro*, **86**, 143–196.

Cunha, P.R.P. (2000) Litostratigrafia do Terciário da região de Miranda do Corvo – Viseu (Bacia do Mondego, Portugal). *I Congresso sobre o Cenozóico de Portugal*. Faculdade de Ciências e Tecnologia, (UNL), Monte da Caparica, 1-4 March, 107–122.

Cunha, P.R.P. and Reis, R.B.P. (1991) Proposta de definição formal de unidades litostratigráficas no registo arcósico, paleogénico e miocénico, do bordo NE da Bacia Lusitaniana - região a NE de Coimbra. *3º Congresso Nacional de Geologia (Resumos)*, Coimbra.

Davis, J.C. (1986) *Statistics and Data Analysis in Geology*. Wiley, New York.

Decleer, J., Ottenburgs, R., Vandenberghe, N., and Viaene, W. (1981) Geological and physico-chemical characterization of

Belgian non-refractory clay deposits and its implications for industrial use. Pp. 699–709 in: *Proceedings of the International Clay Conference* (H.Van Olphen and F. Veniale, editors). Elsevier, Amsterdam.

Dondi, M. (1999) Clay materials for ceramic tiles from the Sassuolo District (Northern Apennines, Italy). Geology, composition and technological properties. *Applied Clay Science*, **15**, 337–366.

Everitt, B. (1977) *Cluster Analysis*, Heinemann Educational Books, Ltd., London.

Fabbri, B. and Dondi, M. (1995) *Caratteristiche e Difetti del Laterizio*. Gruppo Editoriale Faenza Editrice, Faenza.

Fabbri, B. and Fiori, C. (1985) Clays and complementary raw materials for stoneware tiles. *Mineralogica et Petrographica Acta*, **29A**, 535–545.

Fiori, C., Fabbri, B., Donati, F., and Venturi, I. (1989) Mineralogical composition of the clay bodies used in the Italian tile industry. *Applied Clay Science*, **4**, 461–473.

Galan, E., Aparicio, P., Gonzalez, I., and Miras, A. (1998) Contribution of multivariate analysis to the correlation of some properties of kaolin with its mineralogical and chemical composition. *Clay Minerals*, **33**, 65–75.

Galhano C., Rocha, F., and Gomes, C. (1999) Geostatistical analysis of the influence of textural, mineralogical and geochemical parameters on the geotechnical behaviour of the "Argilas de Aveiro" formation (Portugal). *Clay Minerals*, **34**, 109–116.

Gorsuch, R.L. (1974) *Factor Analysis*. W.B. Saunders Company, Philadelphia.

Gorsuch, R.L. (1983) *Factor Analysis*. Lawrence Erlbaum Associates, Hillside, New Jersey.

Jouenne, C.A. (1975) *Traité de Céramiques et Matériaux Mineraux*. Editions Septima, Paris.

Kaiser, H.F. (1958) The varimax criteria for analytical rotation in factor analysis. *Psychometrika*, **23**, 187–200.

Kowalkowski, T., Zbytniewski, R., Szpejna, J., and Buszewski, B. (2006) Application chemometrics in river water classification. *Water Research*, **40**, 744–752.

Kramar, S., Lux J., Mladenović, A., Pristacz, H., Mirtič, B., Sagadin, M., and Rogan-Šmuc, N. (2012) Mineralogical and geochemical characteristics of Roman pottery from an archaeological site near Mošnje (Slovenia). *Applied Clay Science*, **57**, 39–48.

Kumru, M.N. and Bakaç, M. (2003) R-mode factor analysis applied to the distribution of elements in soils from the Aydın basin, Turkey. *Journal of Geochemical Exploration*, **77**, 81–91.

Lisboa, J.V. (2009) *Matérias-primas da Plataforma do Mondego para Cerâmica*. PhD thesis, Univ. Aveiro, Aveiro, Portugal, 247 pp.

Lisboa, J.V. (2014) Argilas comuns em Portugal Continental: ocorrência e caraterísticas. Pp. 135–164 in: *Proveniência de Materiais Geológicos: Abordagens Sobre o Quaternário de Portugal* (P. Dinis, A. Gomes, and S. Monteiro-Rodrigues, editors). APEQ, Coimbra, Portugal.

Lisboa, J.V., Carvalho, J., Cunha, P.R.P., and Oliveira, A. (2013) Typological classification of clayey raw materials for ceramics manufacture, in the Tábua region (central Portugal). *Bulletin of Engineering Geology and the Environment*, **72**, 225–232.

Lisboa, J.V., Oliveira, D.P.S., Rocha, F., Oliveira, A., and Carvalho, J. (2015) Patterns of rare earth and other trace elements in Paleogene and Miocene clayey sediments from the Mondego platform (Central Portugal). *Chemie der Erde*, **75**, 389–401.

Mackenzie, R.C. (1957) *The Differential Thermal Investigation of Clays*. Mineralogical Society, London.

Mackenzie, R.C. (1962) *Differential Thermal Analysis Data Index (with mineral, inorganic and organic sections)*. Cleaver-Hume Press, London.

Maritan, L., Holakooei, P., and Mazzoli, C. (2015) Cluster analysis of XRPD data in ancient ceramics: What for? *Applied Clay Science*, **114**, 540–549.

Marques, R., Dias, M.I., Prudêncio, M.I., and Rocha, F. (2011) Upper Cretaceous clayey levels from western Portugal (Aveiro and Taveiro regions): clay mineral and trace-elements distribution. *Clays and Clay Minerals*, **59**, 315–327.

Martins, R.V.S. (2007) *Investigação Científica e Tecnológica de Matérias-primas Minerais de Santiago do Cacém (Alentejo) e das suas Potencialidades para a Indústria Cerâmica*. PhD thesis, Univ. Aveiro, Aveiro, Portugal, 457 pp.

Mazzoleni, P. and Summa, V. (1996) Compositional characteristics of Plio-Pleistocene clays from Tricarico (Potenza, Southern Italy) and their utilization by the Italian tile industry. *Applied Clay Science*, **11**, 251–268.

Montana, G., Ontiveros, M.A.C., Polito, A.M., and Azzaro, E. (2011) Characterisation of clayey raw materials for ceramic manufacture in ancient Sicily. *Applied Clay Science*, **53**, 476–488.

Oliveira, J.M.S., Moura, A.C., and Grade, J. (1980) Argilas especiais da região de Barracão-Pombal: aplicação da análise matemática multivariada ao seu estudo e caracterização. *Comunicações dos Serviços Geológicos de Portugal*, **66**, 195–208.

Pais, J., Cunha, P.P., Pereira, D.I., Legoinha, P., Kullberg, J.C., Dias, R., Brum, S.A., and Moura, D. (2012) *The Paleogene and Neogene of Western Iberia (Portugal)*. Springer, Berlin, Heidelberg, ISBN: 978-3-642-22400-3.

Pais J., Cunha P.P., Legoinha P., Dias R.P., Pereira D.I., and Ramos A. (2013) Cenozóico das Bacias do Douro (sector ocidental), Mondego, Baixo Tejo e Alvalade. Pp. 461-532 in: *Geologia de Portugal: Vol. II – Geologia Mesocenozóica de Portugal* (R. Dias, A. Araújo, P. Terrinha, and J.C. Kullberg, editors). Escolar Editora, Lisbon.

Papatheodorou, G., Demopouloua, G., and Lambrakis, N. (2006) A long-term study of temporal hydrochemical data in a shallow lake using multivariate statistical techniques. *Ecological Modelling*, **193**, 759–776.

Reimann, C. and Filzmoser, P. (2000) Normal and lognormal data distribution in geochemistry: death of a myth. Consequences for the statistical treatment of geochemical and environmental data. *Environmental Geology*, **39**, 1001–1014.

Rollinson, H. (1993) *Using Geochemical Data: Evaluation, Presentation and Interpretation*. Longman Scientific and Technical. Wiley, New York.

Santos, P.S. (1975) *Tecnologia de Argilas. Vol. 1-Fundamentos* and *Vol. 2-Aplicações* (E. Blucher, editor), University of São Paulo, São Paulo, Brazil.

Schultz, L.G. (1964) Quantitative interpretation of mineralogical composition from X-ray and chemical data for the Pierre Shale. *U.S. Geological Survey Professional Paper*, **391-C**, 1–31.

Sequeira, A.D., Cunha, P.P., and Sousa, M.B. (1997) A reactivação de falhas no intenso contexto compressivo desde meados do Tortoniano, na região de Espinhal-Coja-Caramulo (Portugal Central). *Comunicações do Instituto Geológico e Mineiro*, **83**, 95–126.

Singer, F. and Singer, S. (1963) *Industrial Ceramics, vol. 1 and 2*, Chapman & Hall, Ltd., London.

Singh, K.P., Malik, A., Mohan, D., and Sinha, S. (2004) Multivariate statistical techniques for the evaluation of spatial and temporal variations in water quality of Gomti River (India)-a case study. *Water Research*, **38**, 3980–3992.

Shepard, F.P. (1954) Nomenclature based on sand-silt-clay ratios. *Journal of Sedimentary Petrology*, **24**, 151–158.

https://doi.org/10.1346/CCMN.2016.064040 Published online by Cambridge University Press

Soares, A.F., Marques, J.F., and Sequeira, A.D. (2007) *Notícia Explicativa da Folha 19-D – Lousã*. Geology Department, INETI, Lisbon.

Statsoft (2001) *STATISTICA System Reference*. Statsoft, Inc., 2300 East 14th Street, Tulsa, OK 74104 USA.

Stevens, J. (1986) *Applied Multivariate Statistics for the Social Sciences*. Lawrence Erlbaum Associates, Hillsdale, New Jersey, USA.

Strazzera, B., Dondi, M., and Marsigli, M. (1997) Composition and ceramic properties of Tertiary clays from southern Sardinia (Italy). *Applied Clay Science*, **12**, 247–266.

Thorez, J. (1976) *Practical Identification of Clay Minerals*. Editions G. Lelotte, Belgium.

Ward, J.H. (1963) Hierarchical grouping to optimize an objective function. *Journal of the American Statistical Association*, **58**, 236–244.

Winkler, H.G.F. (1954) Bedeutung der korngröbenverteilung und des mineralbestandes von tonen fiir die herstellung grobkeramischer erzeugnisse. *Berichte der Deutschen Keramischen Gesellschaft*, **31**, 337–343.

Zhu, J., Shan, J., Qiu, P., Qin, Y., Wang, C., He, D., Sun, B., Tong, P., and Wu, S. (2004) The multivariate statistical analysis and XRD analysis of pottery at Xigongqiao site. *Journal of Archaeological Science*, **31**, 1685–1691.

Zhou, F., Liu, Y., and Guo, H. (2007) Application of multivariate statistical methods to water quality assessment of the watercourses in northwestern New Territories, Hong Kong. *Environmental Monitoring Assessment*, **132**, 1–13.

Zhou, J., Ma, D., Pan, J., Nie, W., and Wu, K. (2008) Application of multivariate statistical approach to identify heavy metal sources in sediment and waters: a case study in Yangzhong, China. *Environmental Geology*, **54**, 373–380.

Zorski, T., Ossowski, A., Środoń, J., and Kawiak, T. (2011) Evaluation of mineral composition and petrophysical parameters by the integration of core analysis data and wireline well log data: the Carpathian Foredeep case study. *Clay Minerals*, **46**, 25–45.

(*Received 5 November 2015; revised 19 October 2016; Ms. 1064; AE: S. Kadir*)